Spring 5-2007

Conceptual Modular Reactor Design

Carol Elizabeth Dudney
University of Tennessee - Knoxville

Conceptual Modular Reactor Design

The University of Tennessee
Spring 2007
Instructor: M.L. Grossbeck

Led By: Carol Dudney

Team Members: Justin Belles, Brandon Davis,
Laurel Helton, Michael Sharp, and Stuart Walker

Executive Summary

Many remote regions of the world do not have viable sources of power; nuclear power can provide a long living source of energy which needs relatively little maintenance and infrequent refueling. The goal of this project is to determine the feasibility of producing a modular reactor system which can be transported in pieces over land to remote locations and to present a viable design for this task. The design of a modular 100 MWe nuclear power plant is an involved and elaborate multi-person effort. For the model reactor presented in this report many critical elements normally presented have been left for future work on this project due to the severe time constraints of the design report.

The most promising design prospect for this project is based on the Liquid Metal Fast Breeder Reactor (LMFBR) commercial design. By utilizing the compact size and intrinsically lightweight of the LMFBR system, the project can easily be modified to meet the transportation requirements. The design incorporates a liquid sodium coolant, 19% enriched uranium oxide fuel, and boron carbide control rods. The sodium coolant allows for an overall lighter weight reactor to comparable water reactors. Sodium, like water, allows for the design of a negative void coefficient, a major safety aspect. The 19% enriched uranium oxide avoids many proliferation concerns during transport by staying below the 20% limit. Also in a fast breeder reactor, this fuel allows for fuel conversion, thus prolonging the lifetime of the reactor.

Shielding concerns will primarily be dealt with by entrenching the reactor vessel and related systems under ground. A large retractable slab will cover the top to protect personnel and avoid sky shine. The control, secondary, and auxiliary systems will all be housed above ground inside the plant systems building. Other safety concerns, such as a Loss of Coolant and Loss of Flow Accidents are also addressed within the report.

The report also deals with the heat transfer properties of the primary and secondary systems. A modified gas turbine system operating on a closed loop Brayton cycle fulfills the power conversion needs of the system. By circulating an inert gas such as helium, the highly chemically reactive nature of liquid sodium can be overcome. The gas turbine system also eliminates many of the heavy and cumbersome systems associated with steam turbine systems. The turbine system will connect and reject heat to large, truck based radiators, the system's ultimate heat sink.

Each subsystem of the plant is designed such that each one can easily be mounted and transported by standard shipping freights. Thus one can conclude that the proposal for a modular, transportable, 100 MWe reactor system is not only feasible, but practical. The design proposal submitted in this report meets all General Design Criteria, as well as meeting the project specific guidelines.

TABLE OF CONTENTS

LIST OF FIGURES....4
LIST OF TABLES....4
INTRODUCTION....5
LIQUID METAL FAST BREEDER REACTOR BACKGROUND....5
REACTOR CORE....10
FUEL....11
INITIAL COOLANT....11
INITIAL CORE GEOMETRY....12
NEUTRON TRANSPORT....13
NEW CORE GEOMETRY AND COOLANT....13
SCALE....14
VOID COEFFICIENT....15
TEMPERATURE COEFFICIENT....16
CONTROL RODS....17
DOSE CALCULATIONS....18
HEAT TRANSFER....20
THERMAL HYDRAULIC DESIGN METHODOLOGY....20
THERMODYNAMIC PROPERTIES OF THE FUEL....20
FUEL PIN....22
CLADDING TEMPERATURES....24
COOLANT TEMPERATURE....25
PUMP POWER....26
NATURAL CIRCULATION....27
SECONDARY SYSTEM....29
SAFETY....34
SHIELDING....34
PASSIVE SAFETY SYSTEM....36
LOSS OF COOLANT ACCIDENT....36
LOSS OF FLOW ACCIDENT....37
OTHER DESIGN CRITERIA....38
HEAT SINK....38
AUXILIARY HEATERS....38
TRANSPORTATION....39
CONCLUSIONS....40
FUTURE WORK....43
REFERENCES....46
APPENDIX A: NORMAL OPERATING SCALE INPUT DECK....47
APPENDIX B: VOID COEFFICIENT DETERMINATION SCALE INPUT DECK....49
APPENDIX C: TEMPERATURE COEFFICIENT DETERMINATION SCALE INPUT DECK....51
APPENDIX D: ENSURING SHUTDOWN CAPABILITY OF REACTOR SCALE INPUT DECK..53
APPENDIX E: NORMAL OPERATING DOSE CALCULATIONS SCALE INPUT DECK....55
APPENDIX F: TRANSPORTATION DOSE CALCULATION SCALE INPUT DECK....56
APPENDIX G: LOCA ANALYSIS SCALE INPUT DECK....57
APPENDIX H: HEAT TRANSFER MATLAB CODE....59
APPENDIX I: BRANDON HOLDEN'S MATLAB PROGRAM....62
APPENDIX J: DESIGN PROJECT DEFINITION....65

List of Figures

Figure 1: LMFBR Loop vs. Pool Design.....8
Figure 2: Initial Spherical Core Geometry.....12
Figure 3: Close-Up of Fuel Plates in Initial Design.....12
Figure 4: Normal Operating K_{EFF}.....15
Figure 5: Fuel and Cladding Temperatures as a Function of Vertical Position Within the Core.....24
Figure 6: Plot of Pump Power as a Function of the Dimensionless Value L/D.....27
Figure 7: The Change in Density as a Function of the Dimensionless Parameter L/D.....28
Figure 8: Plot of the Maximum Pipe Length to Allow Natural Circulation Versus Pipe Diameter for Several L/D Values.....29
Figure 9: SGT-800 Industrial Gas Turbine – 45 MW.....31
Figure 10: Closed Loop Brayton Cycle.....33
Figure 11: Visual Representation of the Reactor's Shielding.....35
Figure 12: Basic Shell and Tube Heat Exchanger.....38
Figure 13: ROGERS® 100 Ton Lowboy.....39

List of Tables

Table 1: Properties of Uranium-235.....11
Table 2: Properties of Sodium.....14
Table 3: Void and Temperature Coefficient Case Comparison.....17
Table 4: K_{EFF} Shut-Down to Normal Comparison.....18
Table 5: Dose Rates for Normal Operating and Transportation Cases.....19
Table 6: Miscellaneous Core Properties.....21
Table 7: Various Material Properties of the Fuel.....22
Table 8: Material Properties of Cladding.....24
Table 9: SGT-800 Industrial Gas Turbine Technical Specifications.....32
Table 10: Theoretical Closed Loop Gas Turbine Technical Specifications.....33
Table 11: Properties of Helium.....34
Table 12: Determination of Safe Shutdown with a LOCA.....37
Table 13: Reactor Parameters.....42

Introduction

This year's design project was to design a reactor that was transportable, modular, and operable in remote locations. Due to the long fuel cycles possible with Liquid Metal Fast Breeder Reactors, several of these designs were researched and discussed. Originally, a spherical reactor with disk shaped fuel plates was attempted, but a cylindrical reactor using fuel pins was the result of the groups planning and research.

There were only two basic design criteria taken into account for this project. First, one hundred Megawatts electric power was required. The second criterion was that the life cycle last between twenty and thirty years. Typical nuclear reactors operate approximately 50-60 years on several fuel loads before decommissioning. Furthermore, the reactor design should not include any fuel reloading. To accomplish this, the initial k-effective should be higher than normally desired, thus specific attention is required as to the safe transport of the reactor. Finally, the reactor must be of a manageable mass so that it is transportable by truck. The idea is that fabrication of all the components will occur in the United States. From the U.S.A. the components of the plant will be transported to the desired location, set up, and local operators trained on its operation.

Liquid Metal Fast Breeder Reactor Background

First created in the 1950s, Fast Breeder Reactors (FBRs) are a variant on the more widely used thermal nuclear reactors as used in Boiling Water and Pressurized Water Reactor systems (BWR and PWR, respectively). As the name implies, FBR technology utilizes the fast spectrum of neutrons to 'breed' fissile fuel from fertile material, unlike the

typical reactors, which function solely on the slower thermal spectrum. In order to keep the neutron spectrum at the higher energy level, the FBRs use a coolant that does not moderate the neutrons, frequently some form of liquid metal. The first experimental breeder reactor was a small plutonium-fueled, mercury-cooled device, operating at a power level of 25 kW. A breeder, cooled with a mixture of sodium and potassium, was placed in operation in 1951 at the Argonne National Laboratory in Idaho [3]. This reactor, the Experimental Breeder Reactor-I (EBR-I), produced 200 kW of electricity, the world's first nuclear-generated electricity [6]. Since these early experiments, several Liquid Metal Fast Breeder Reactors (LMFBRs) have been or are currently under construction around the world.

Most LMFBRs operate on the uranium-plutonium fuel cycle or thorium-U-233 fuel cycle. Reactors are typically fueled with isotopes of plutonium in the core with a blanket of natural or depleted uranium. Because fission neutrons emitted per neutron absorption increases with neutron energy (for energies above ~100 keV), the breeding ratio of Pu-239 also increases with energy. This is the driving idea behind preventing the moderation of fission neutrons in a fast reactor. This excludes lightweight nuclei from the core and forces the use of non-moderating coolants, such as liquid sodium metal.

With an atomic weight of 23 amu, sodium does not appreciably slow neutrons through scattering. Furthermore, since sodium has excellent thermal conductivity, reactors are operable at extremely high power densities. This allows LMFBR cores to be relatively compact. Additionally, because sodium has a very high boiling point, reactor coolant loops are operable at high temperatures without the need for high pressures to prevent boiling, thus no heavy pressure vessel is required. This high coolant temperature leads to

high-temperature, high-pressure steam, and thus to high plant efficiency. Finally, sodium, unlike water, is not corrosive to many structural materials. Reactor components immersed in liquid sodium for years suffer minimal damage from the coolant. However, this use of sodium also has some negative qualities. Sodium's melting point is much higher than room temperature, so the entire coolant system requires heaters to prevent the sodium from solidifying. These heaters are utilized at startup and times of low reactor power by a spiral of heating wire running along coolant piping, valves, and so forth. Sodium is also highly chemically reactive and can become radioactively activated from prolonged exposure to the reactor core. Because hot sodium reacts violently when exposed to air or water, the sodium is isolated from the rest of the environment by multiple layers of safety features. This separation also lends to LMFBRs being inherently tight systems that emit far less radiation to the environment than comparable Thermal Reactors.

Most LMFBRs have two sodium loops: the primary reactor loop carrying radioactive sodium and an intermediate sodium loop containing inactivated sodium, which carries the heat from the primary loop via an intermediate heat exchanger to the steam generator. There are two types of intermediary loops used in modern LMFBRs, the loop-type LMFBR and the pool-type LMFBR, as seen in Figure 1. The loop-type, except for the presence of the intermediate loop, differs insignificantly in design from a PWR. All primary loop components, the reactor, pumps, heat exchangers, and so on, are separate and independent. However, substantial amounts of shielding are required around all the primary loops in a loop-type plant, making these plants large, heavily built buildings. By contrast, in a pool-type LMFBR no radioactivity leaves the reactor vessel, so no other

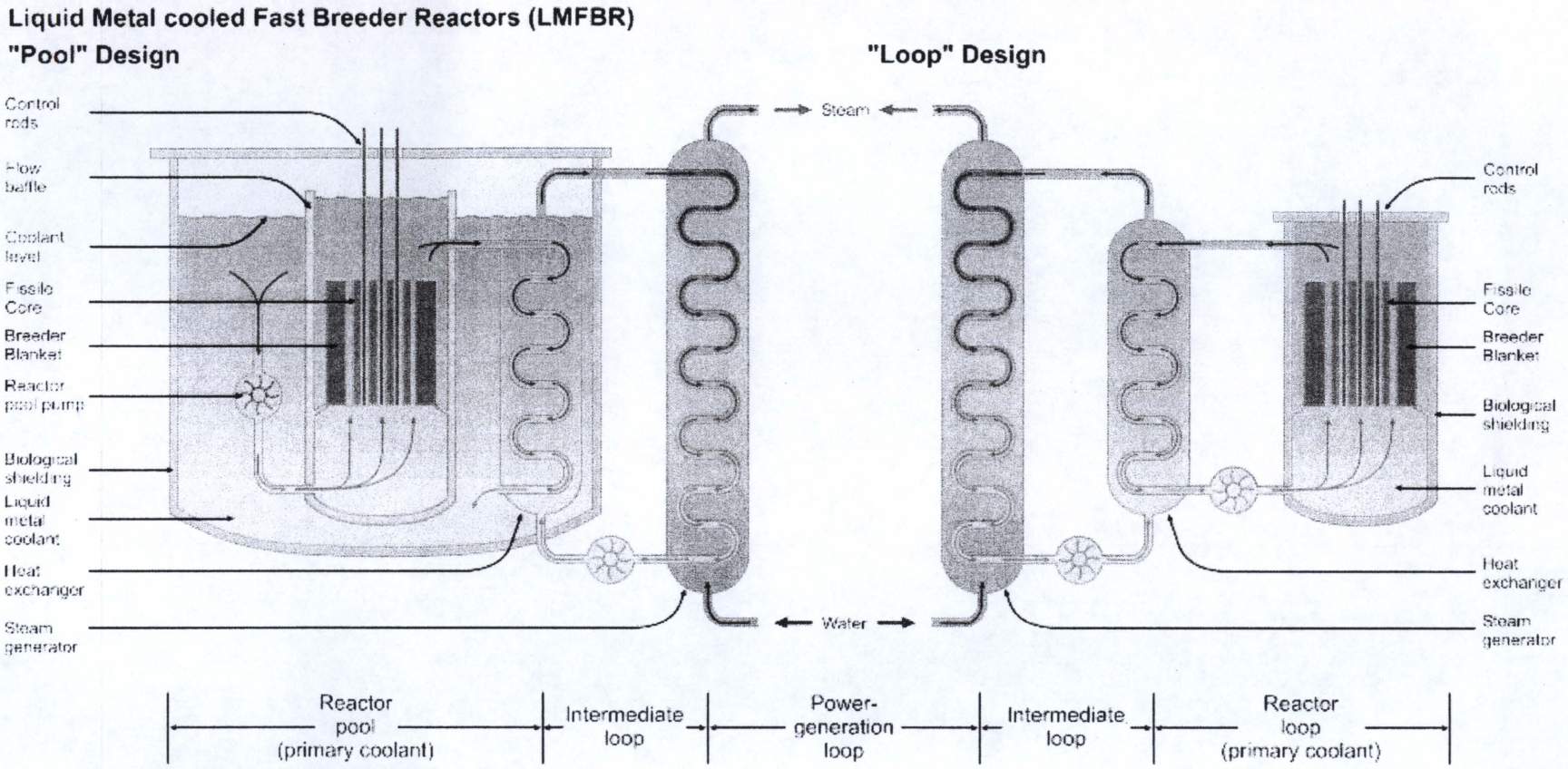

Figure 1: LMFBR Loop vs. Pool Design

component of the plant requires heavy shielding. In addition, the usual practice is to locate pool-type reactor vessels in-ground, so that only the uppermost portion of the vessel requires heavy shielding. It is possible to walk into the reactor room where a pool-type reactor is operating and even walk across the top of the reactor without receiving a significant radiation dose. This type of LMFBR is safe and compact.

In general, the core of a LMFBR consists of an array of fuel assemblies, which are hexagonal or square stainless steel arrays 10 to 15 cm across and 3 or 4 m long that contain the fuel and fertile material. An assembly for the central region of the reactor contains fuel pins at its center and blanket pins at either end. Assemblies for the outer part of the reactor contain only blanket pins. When these assemblies are placed together, the effect is to create a central cylindrical driver surrounded on all sides by the blanket. The fuel pins are commonly stainless steel clad pellets 6 or 7 mm in diameter composed of a mixture of oxides of plutonium and uranium. The equivalent enrichment of the fuel ranges from 15% to 35% plutonium. The fuel pins are separated by spacers or in some cases by wire wound helically along each pin. The pins in the blanket, which contain only uranium dioxide, are larger in diameter, about 1.5 cm, because they require less cooling than the fuel pins. Both fuel and blanket pins are more tightly packed in a LMFBR than in a thermal water reactor, because the heat transfer properties of sodium are better than those of water. The liquid sodium coolant enters through holes near the bottom of each assembly, passes upward around the pins, removing heat as it goes, and then exits at the top of the core [8].

Although virtually all present day LMFBRs operate with uranium-plutonium oxide fuel, there is considerable interest in the future use of fuel composed of uranium-plutonium

carbide, since large breeding ratios are possible with this fuel. This is due to the fact that while there are two atoms of oxygen per atom of uranium in the oxide, there is only one atom of carbon per uranium atom in the carbide. Light atoms such as carbon and oxygen tend to moderate fission neutrons. Since there fractionally fewer of these atoms in the carbide than in the oxide, it follows that the energy distribution of neutrons in a carbide-fueled LMFBR is shifted to higher energies than in a comparable oxide-fueled LMFBR [8]. However, carbide fuel is more difficult to fabricate and achieves a burn up value half that of oxide fuels. Therefore making oxide fuels more desirable fuel form [7].

LMFBR's compact size along with their ability to produce, or breed, new fuel makes LMFBRs a highly desirable reactor type. They exhibit long fuel cycles and little environmental impact compared to an equivalently sized output coal plant. As the need for long-lived fuel sources presses on the world's resources, LMFBRs offer an appealing option that should only become more popular in the future.

Reactor Core

The path leading to the current group design was a lengthy and involved process. The reactor could potentially be placed anywhere, and that required a design that was flexible as well as adaptable. The core also needed to last for several years. It was this last design consideration that led to a fast reactor concept.

Fuel

In order to maximize the fuel lifetime of the reactor, a 19% enriched uranium dioxide fuel is used. The 19% U-235 level is low enough to avoid proliferation concerns during transport, while at the same time allowing for fuel conversion during the life cycle of the reactor. Fuel pins are stainless steel clad, with sodium filling the gap between the fuel and the cladding. Uranium is a standard fuel in many reactors world wide, and is thus well understood with a well-documented behavior. Table 1 below gives a partial list of the properties of Uranium.

Table 1: Properties of Uranium-235

Atomic Mass	235.0439231amu
Half life	703,800,000 years
Average Energy Released per Fission	~200 MeV

Initial Coolant

A fast reactor is the best concept to utilize for long-lived cores, as it converts fertile fuel into fissile fuel. This allows for a longer lifetime without having high initial fuel enrichment. For coolant, a liquid metal is the most attractive option. Liquid metals do not moderate neutrons the way water does. Utilizing water as a coolant would also require the use of a pressure vessel. The mass of a pressure vessel would limit the number of transportation options. The drawback to a liquid metal coolant is the need for an auxiliary heating system that would only be used in reactor startup.

Metals tend to be solid at room temperature, with the exception of mercury. This metal is toxic and can cause serious environmental issues, yet remains attractive to designers of

fast reactors due to its low melting point. Other options for metal coolants include lead, lead bismuth, or sodium. All of these have the common reactor startup problem of being solids at room temperature. In an attempt to avoid the problem of designing an auxiliary system just for the initial startup of a reactor, a mercury coolant was chosen. In addition, mercury was selected over the other coolant options due to lead's slightly larger mass and the combustion problems associated with sodium. With the coolant and reactor type now in mind, core geometry was the only factor remaining that required discussion.

Initial Core Geometry

The neutron economy is a limiting factor when attempting to get a core to operate for the maximum desired time span of thirty years. Therefore, a spherical core geometry was attempted in order to reduce neutron leakage and consequently reduce fuel consumption, as seen in Figure 2. Fuel pins were initially discussed but the idea of circular fuel plates traversing the entire diameter of the core, as seen in Figure 3, was considered an idea worth trying. Fuel plates give a well-defined flow path for the coolant and limit the amount of moderation that could occur from the coolant.

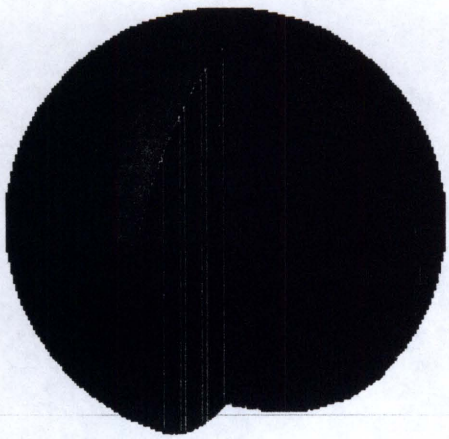

Figure 2: Initial Spherical Core Geometry

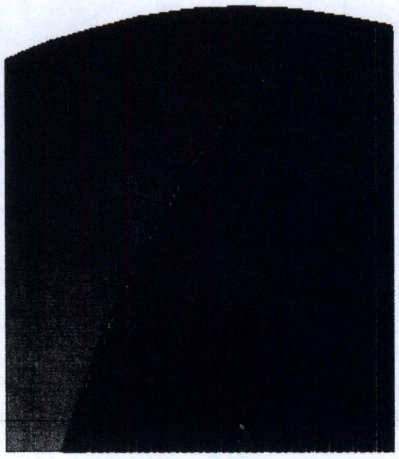

Figure 3: Close-up of Fuel Plates in Initial Design

Neutron transport

Utilizing the above information, the team went to work with SCALE 5.0 and 5.1. A spherical core with the plate fuel was easily constructed, as had been discussed. However, difficulties arose while attempting to input the mercury coolant. SCALE returned an error every time the mercury was inserted into the input deck. After speaking with Dr. Pevey, the SCALE expert at the University of Tennessee, the conclusion was reached that the cross section data for mercury is not in the libraries used by SCALE. This unfortunate news required the initiation of a new design.

New Core Geometry and Coolant

Now back to square one and a couple weeks of research and effort wasted, it was decided to keep the design simple and get a basic core operating for the desired time span and then if further time permitted to go back and begin adding embellishments. Our past research led us to a relatively simple cylindrical geometry with fuel pins, a concept upon which almost all commercial reactors are based. This also reduced the workload on the thermal analysis team, who were going to be doing hard work attempting to analyze a spherical core with fuel plates. We also switched from our mercury coolant over to sodium due to the primary fact that it has the lowest melting point of the other coolant options [1].

Sodium coolant is a tested and understood coolant in fast breeder reactors. Sodium has a small neutron cross-section allowing neutrons to be scattered back into the fuel with

negligible moderation. In addition, sodium has excellent thermal properties and is less dense than water, thus reducing the overall weight of the system. Use of sodium also allows for the design of a negative coefficient of reactivity within the reactor core. Sodium does present a challenge with its high level of chemical reactivity, but this is over come by other engineered safety features in the power plant. Table 2 shows a partial list of some of the pertinent properties of sodium.

Table 2: Properties of Sodium

Atomic Weight	22.98976928
Solid Density	968 kg m^{-3}
Speed of Sound	3200 m s^{-1}
Melting Point	97.72 °C
Thermal Conductivity	63 W m^{-1} K^{-1}

SCALE

Finally, with the new core geometry in mind, SCALE was again utilized in modeling the core neutronics. Using the SAS2H sequence, we were able to do a simple calculation on the lifetime of our reactor and the basic dimensions. After several iterations of the design process, we were able to obtain our current design, the input deck of which can be seen in Appendix A. Approximately 88.75" in diameter and 82" in height, our cylindrical reactor core loaded with 19 wt. % UO_2 would run for over 27 years (10,000 days) at 500 MW^{th}. All that was left was to determine if the reactor had a negative void coefficient and a negative temperature coefficient, important considerations before constructing any reactor. A graphical representation of K_{eff} vs. the operating timeline can be seen below in Figure 4.

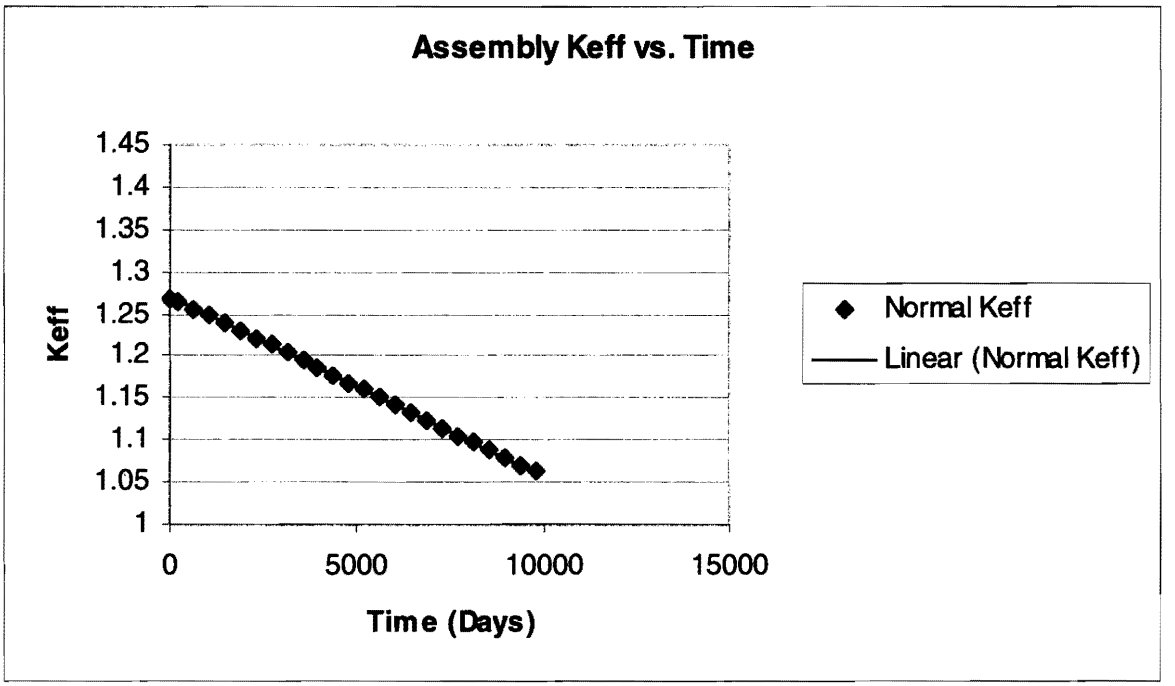

Figure 4: Normal Operating K_{eff}

Void Coefficient

The void coefficient, a_V, is a measure of the number of neutrons the coolant will absorb. Reactor designs require a negative void coefficient to maintain a stable reactor.

$$a_V = \frac{1}{k}\frac{dk}{dV}$$

Meaning, if coolant is lost the reactivity will decrease [2].

Determining the void coefficient would not be difficult. The density of the sodium coolant was reduced from the normal density and the case was run using SCALE5.1. The input deck for the reduced sodium density case can be viewed in Appendix B. The normal and reduced sodium density outputs were then compared. From the side by side comparison of the outputs in Table 3, it is clear the decreased sodium density initially

caused a slight reduction in K_{eff}. However, it is noted that at approximately 2,708 days, the void coefficient becomes positive. This phenomenon will need further exploration. It is potentially a problem with the number of times the burnup was calculated throughout the core modeled lifetime. This would be a cumulative effect, potentially affecting the void coefficient as it has. The cost of running more burnup libraries would be extremely high, as we do not have large computing power on personal pcs. With that information in mind, it is our belief that a more detailed analysis will reveal a negative void coefficient throughout the reactor life.

Temperature Coefficient

Further SCALE manipulations were exploited to determine the temperature coefficient. The temperature coefficient, as defined by [2]:

$$\alpha_T^F \equiv \frac{1}{k}\frac{dk}{dT_F},$$

must be negative to show that the reactor will be inherently stable during fuel temperature fluctuations. To test the design for a negative temperature coefficient, the temperature of the fuel, as specified in the SCALE input deck, was lowered 500 K. This reduced temperature input deck can be viewed in Appendix C. If the design had a negative temperature coefficient, the reduced UO_2 temperature should result in an increase in K_{eff}. The results were again viewed side by side in Table 3, and it was clear that initially this resulted in a higher K_{eff}. However, it was noted that towards the end of the core lifetime, at approximately 8,542 days it resulted in a lower K_{eff}. This was also the case with the void coefficient. As with the void coefficient, it is our belief that a more detailed analysis

will reveal a negative temperature coefficient throughout the reactor life. All that remains now is to determine if the reactor could be safely shut-down with the number of control rods included and how much shielding is required to safely operate the reactor.

Table 3: Void and Temperature Coefficient Case Comparison

K_{eff} for Coefficient Determination			
Days	Normal	Void Coefficient	Temperature Coefficient
0	1.2683	1.2663	1.2699
208	1.2641	1.2622	1.2657
625	1.2557	1.2541	1.2573
1042	1.2472	1.246	1.2487
1458	1.2387	1.2377	1.2401
1875	1.2301	1.2294	1.2314
2292	1.2214	1.2211	1.2227
2708	1.2126	1.2126	1.2138
3125	1.2038	1.2041	1.2049
3542	1.1949	1.1955	1.196
3959	1.186	1.1869	1.187
4375	1.177	1.1782	1.1779
4792	1.168	1.1695	1.1688
5209	1.159	1.1608	1.1597
5625	1.1499	1.152	1.1506
6042	1.1409	1.1433	1.1414
6459	1.1319	1.1346	1.1323
6875	1.1229	1.1258	1.1232
7292	1.114	1.1172	1.1142
7709	1.1051	1.1085	1.1052
8126	1.0963	1.0999	1.0963
8542	1.0875	1.0914	1.0874
8959	1.0789	1.083	1.0787
9376	1.0703	1.0747	1.07
9792	1.0619	1.0664	1.0615

Control Rods

Aside from void and temperature coefficients, it must be determined if the 4,802 boron control rods included in the design are enough to stop the reactors chain reaction. This

analysis was completed using the SAS2H sequence in SCALE, which runs BONAMI, NITAWL, XSDRN, COUPLE, and ORIGEN. The SCALE input deck can be viewed in Appendix A. It can be seen in Table 4 below that the reactor can be safely shut down utilizing the 4,802 control rods consisting of 36% B-10 and 64% B-11.

Table 4: K_{eff} Shut-Down To Normal Comparison

K_{eff} for Safe Shut Down		
Days	Normal	Shut-Down
0	1.2683	0.8507
208	1.2641	0.9825
625	1.2557	0.9802
1042	1.2472	0.9777
1458	1.2387	0.9752
1875	1.2301	0.9727
2292	1.2214	0.9702
2708	1.2126	0.9677
3125	1.2038	0.9652
3542	1.1949	0.9627
3959	1.186	0.9601
4375	1.177	0.9575
4792	1.168	0.9549
5209	1.159	0.9523
5625	1.1499	0.9497
6042	1.1409	0.947
6459	1.1319	0.9444
6875	1.1229	0.9417
7292	1.114	0.939
7709	1.1051	0.9363
8126	1.0963	0.9336
8542	1.0875	0.9309
8959	1.0789	0.9282
9376	1.0703	0.9255
9792	1.0619	0.9227

Dose Calculations

It was determined that the SAS1X sequence could do what was required to calculate the dose by running BONAMI, NITAWL, XSDRN, and XSDOSE. A difficulty arose when

attempting to use this sequence with cylindrical geometry. SCALE simply would not run. After a few days and several attempts to remedy the problems, a brainstorming session led to the belief that in order to be conservative we would use a spherical arrangement that had the same volume as our reactor core. This would be the worst case scenario dose estimation if the fuel were to melt and become spherically shaped.

Two issues needed to be addressed to arrive at dose estimation in units of mREM/hr. The dose output from SCALE was normalized to one fission atom being produced. This factor had to be multiplied by the number of fissions per hour in order to calculate the dose. For the normal case this was roughly estimated by unit conversion of 500 MW^{th} to fissions per hour utilizing the conversion of approximately 200 MeV per fission (arriving at an answer of $5.6x10^{22}$ fissions/hr). For the transportation dose estimate, the number of fissions occurring per hour was determined by the spontaneous fission rates of both uranium-235 and uranium-238 (arriving at an answer of $1.25x10^{9}$ fissions/hr). The second issue needing to be addressed was what an acceptable dose level was on the outside of the reactor core. Since the reactor needs operators on site it was decided that 0.5 mREM/hr was the maximum dose we would allow on the surface of the shielding. This will allow operators safe working conditions within a close proximity to the reactor core itself. The dose rates in mREM/hr for both the normal operating case and the transportation case can be viewed in Table 5 below. The shielding used to reduce these rates is discussed in more detail in the shielding section.

Table 5: Dose Rates for Normal Operating and Transportation Cases

	Normal	Transportation
Total Neutron + Gamma Dose:	(mREM/hr)	(mREM/hr)
Detector 1 (sphere surface)	0.46	0.41

Heat Transfer

Thermal Hydraulic Design Methodology

The general design methodology of the thermal hydraulic aspects of a portable liquid metal cooled reactor was to analyze core temperatures at 500 MWt assuming a constant radial heat generation rate and a sinusoidal axial heat generation rate. The axial heat generation rate is given by [10]:

$$q'(z) = q_0' \cos \frac{\pi z}{L_e}$$

Where $q'(z)$ is the heat addition rate, q_0' is the peak linear heat-generation rate, L_e is the length over which the neutron flux has a nonzero value, and z is the vertical position. The fuel temperatures were utilized to calculate the temperature of the coolant that was used in order to find the pumping power needed to circulate the liquid metal coolant.

Various power and core geometry parameters used in this analysis are listed in Table 6.

All results were generated using various models coded in MatLab 6.5 2006a. Height steps of 0.001 m were used to solve the axial temperatures, which will be explained in the next section.

Thermodynamic Properties of the Fuel

There are three main reasons to analyze the thermodynamic properties of the fuel elements. The first reason is to understand temperature gradients, which control thermal stress/strain. The second is that the temperature controls chemical reactions and diffusion processes. Finally, because of the temperature effect on nuclear reaction rates, the fuel temperature depends on heat generation rate within the fuel pin, material properties of the

fuel, coolant and cladding temperature. In order to decouple the temperature field surrounding the fuel element from the neutronics, the heat generation rate should be assumed to be in steady state. Since the fuel can be assumed incompressible along the temperature gradient, the radial heat conduction equation reduces to a steady state solution and therefore decouples itself from the neutronics.

Table 6: Miscellaneous Core Properties

Power and Geometric Properties			
Power		Geometry	
Total Thermal Power (MW)	500	Core Height (m)	2.0828
Total Electrical Power (MW)	100	Core Radius (m)	2.25425
Maximum Linear Power (W/m)	3500	Extrapolated Core Length (m)	2.107
Core Inlet Temperature (K)	653	Core Depth (m)	3
Delta T (K)	300	Pitch (cm)	0.7374
		Fuel Radius (cm)	0.29
		Cladding Gap (cm)	0.012
		Cladding Thickness (cm)	0.038

For solids, thermal conductivity, k, is a function of temperature while pressure has little effect. For UO_2 pellets, k decreases with increasing temperature until about 1230 K then k increases. With increased porosity in the fuel element, thermal conductivity is

decreased. PuO_2 content has a large effect as well. As a result of burn-up, k decreases due to irradiation.

There are several methods to calculate thermal conductivity, k. First, if the thermal conductivity changes little within the temperature range, k may be assumed constant. Secondly, if the change in thermal conductivity is large over the temperature range a mean k may be chosen. Lastly for a more formal solution, k can be assumed to fit an empirical form in which the heat conduction equation reduces to a linear ordinary differential equation in k^2. The thermal conductivity for this design was taken as the average thermal conductivity over the temperature range in needed.

Various material properties of the UO_2 fuel material are included in Table 7.

Table 7: Various Material Properties of the Fuel [10]

Fuel Type	UO_2
Thermal Conductivity, (W/m°K)	3.3
Melting Temperature, (K)	3070
Density, (Kg/m^3)	9.67×10^3

Fuel Pin

The fuel pin was analyzed at the centerline and at the outer surface of the pellet. The centerline temperature is the maximum temperature and therefore must not exceed the melting point of the fuel listed in Table 7. The centerline temperature was calculated by

solving an energy balance axially for a single-phase coolant channel. The centerline temperature was calculated as a function of height in the core according to [10]:

$$T_{cl}(z) = T_{in} + q_0^{'}\left[\frac{L_e}{\pi \dot{m} c_p}\left(\sin\frac{\pi z}{L_e} + \sin\frac{\pi L}{2L_e}\right) + \left(\frac{1}{2\pi R_{co} h} + \frac{\ln(R_{co}/R_{ci})}{2\pi k_c} + \frac{1}{2\pi R_g h_g} + \frac{1}{4\pi k_f}\right)\cos\frac{\pi z}{L_e}\right]$$

The fuel pin outer surface temperature was analyzed using a 1-D radial heat conduction equation for a cylindrical geometry. Using the assumption of constant thermal conductivity the heat conduction equation reduces to [10]:

$$T_{avg} - T_{fo} = \frac{1}{2}(T_{\max} - T_{fo}) = \frac{q^{'}}{8\pi k}$$

The temperature of the fuel is displayed in Figure 5 as the blue line. The minimum temperature was 687.3 K at h = -1.06m. The maximum temperature was 1079 K at h = 0.46m. The temperature at the exit of the core, h = 1.06m, was 986.8 K. Therefore, the temperature difference across the core, with a coolant velocity of 0.97m/s, is 299.5 K. This proves the flow rate of 0.97m/s is a valid flow rate for a LMFBR.

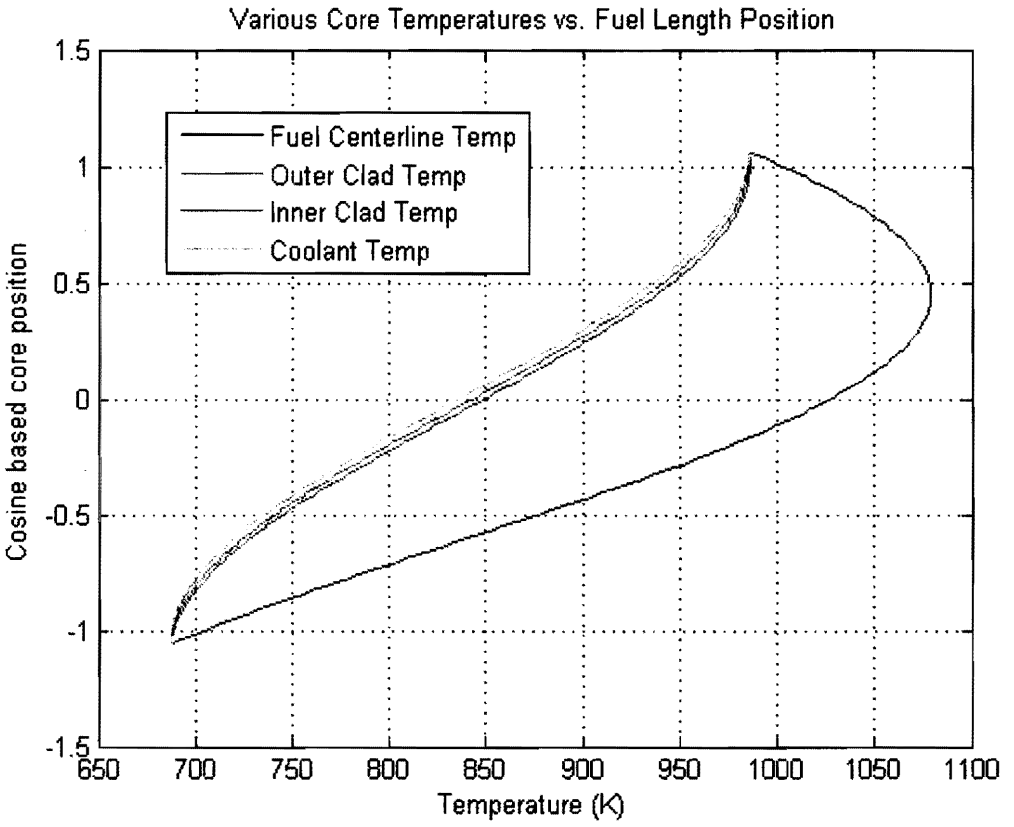

Figure 5: Fuel and cladding temperatures as a function of vertical position within the core [5].

Cladding Temperatures

The cladding material used was type 316 stainless steel (SS-316). Several material properties of SS-316 are listed in Table 8.

Table 8: Material Properties of Cladding

Type	SS-316
Thermal Conductivity, (W/mK)	21.5
Melting Temperature, (K)	1670
Density, (Kg/m^3)	7.80×10^3

The inner surface temperature of the cladding was assumed to be equal to that of the outer fuel surface due to the use of a bonded fuel. By considering the heat flux at the cladding outer surface the temperature of the outer surface of the cladding, $T_{co}(z)$, can be calculated according to [10]:

$$T_{co}(z) = T_{in} + q_0^{'}\left[\frac{L_e}{\pi \dot{m} c_p}\left(\sin\frac{\pi z}{L_e} + \sin\frac{\pi L}{2L_e}\right) + \left(\frac{1}{2\pi R_{co} h}\right)\cos\frac{\pi z}{L_e}\right]$$

Where R_{co} is the outer radius of the cladding, L is the height of the physical core, and L_e is the extrapolation height of the core.

The inner cladding temperature was described as the outer surface temperature of the fuel. The outer cladding surface temperature was calculated according to the above equation, and is given as the red curve in Figure 5. The minimum temperature was 687.3 K at h = -1.06 m. The maximum temperature was 986.2 K at h = 1.0 m. The temperature at the exit of the core was 985.6 K.

Coolant Temperature

The bulk coolant temperature, $T_m(z)$, can be calculated using the same energy balance as the fuel centerline temperature. Given the single phase flow and the temperature independent nature of the material properties the energy balance may be written as [10]:

$$T_m(z) = T_{in} + q_0^{'}\left[\frac{L_e}{\pi \dot{m} c_p}\left(\sin\frac{\pi z}{L_e} + \sin\frac{\pi L}{2L_e}\right)\right]$$

The coolant temperature within each channel was found as a function of height. The sinusoidal shape of the heat generation rate accounts for the S-shape of Figure 5. The minimum temperature was 687.3 K at h = -1.06 m. The maximum temperature was 985.6 K at h = 1.06 m.

Pump Power

The pumping power may be calculated using a momentum balance. Form losses are to be ignored while hydrostatic head losses through the core and shielding will be accounted for. Frictional head losses within the pipe will be accounted for as a function of the dimensionless parameter L/D.

The pumping power, $\dot{W}$, was calculated using the following equation [10]:

$$\dot{W} = \dot{m}\, g(\Delta z + f_{iL} \cdot \left[\frac{L}{D}\right])$$

Where $\dot{m}$ is the mass flow rate, Δz is the change in vertical position, and f is the friction factor. The friction factor was calculated using the equations below[10]:

$$C = a + b_1(P/D - 1) + b_2(P/D - 1)^2$$

$$f_{iL} = C/\mathrm{Re}_{iL}$$

Where C is the friction factor constant, P/D is the pitch to diameter ratio, and Re_{iL} is the Reynolds number for internal losses.

The pump power is plotted as a function of L/D in Figure 6. Given an assumed total pipe length of 50m and an average pipe diameter of 10cm a reasonable L/D value of 500 is found. The pumping power required to overcome these losses is found to be 23.85 kW, which is well below the 100 MWe generated.

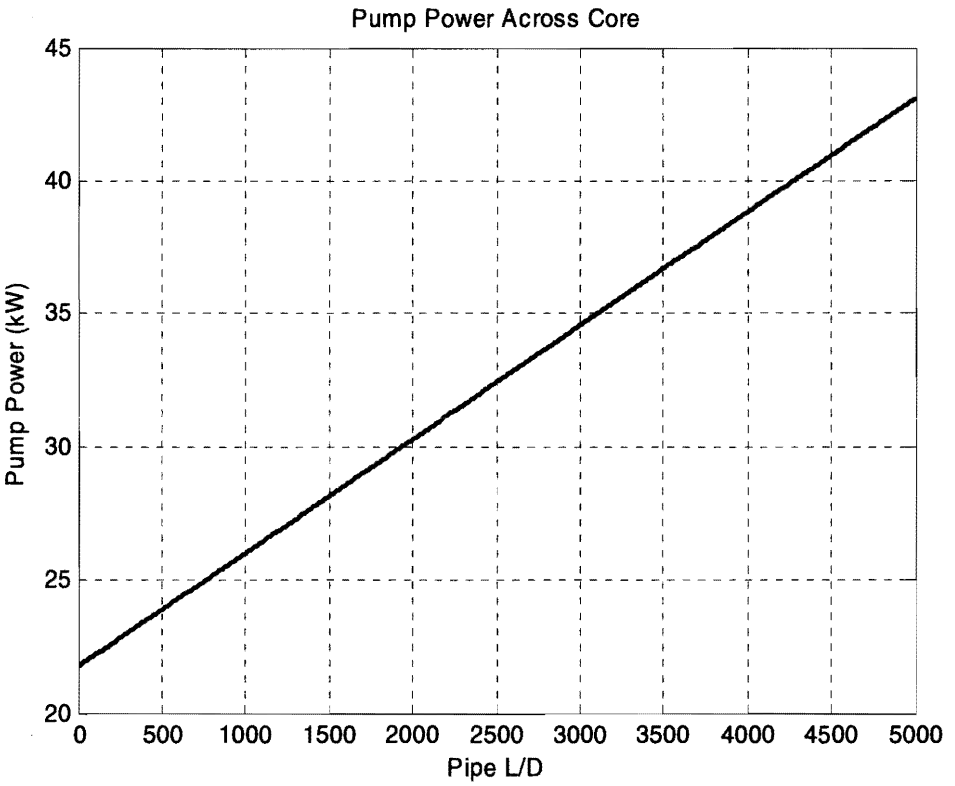

Figure 6: Plot of pump power as a function of the dimensionless value L/D.

Natural Circulation

A very important design criterion is that natural circulation of the coolant be sufficient to remove the decay power after the core is shutdown. The fractional power after shutdown is taken as 10% of the total thermal power. The density gradient causes a buoyant force, which drives the natural circulation of the coolant. This density gradient, $\Delta\rho$, is defined using the following equation [10]:

$$\Delta\rho = \frac{\bar{\rho} v^2 f}{g\Delta h} \cdot \left[\frac{L}{D}\right]$$

The density gradient was then scaled through a linear interpolation to get a temperature gradient. Then general heat conduction equations were solved to get the total required area of heat transfer. By varying the diameter of the piping a maximum pipe length can be solved for.

Natural circulation was modeled as a function of the dimensionless value L/D. Figure 7 shows the solution of the above equation for $\Delta\rho$. Secondly, for various L/D values the diameter versus maximum length was plotted in Figure 8. Notice as the surface area drops with diameter so too does the maximum pipe length needed for the heat exchanger.

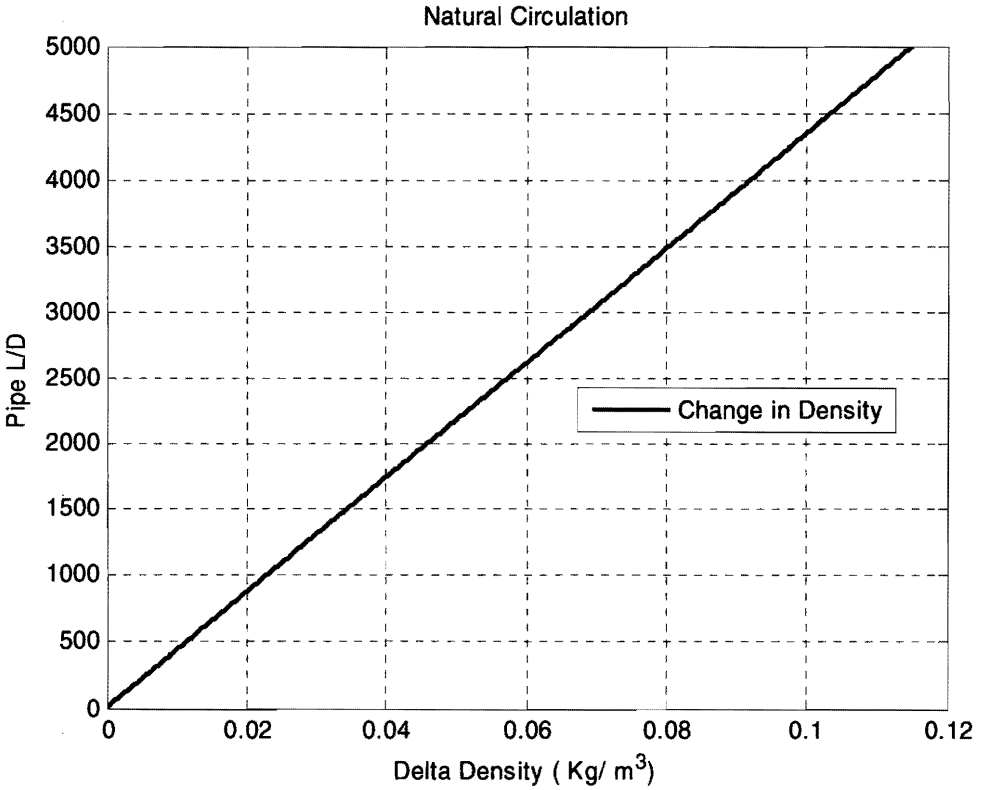

Figure 7: The change in density as a function of the dimensionless parameter L/D.

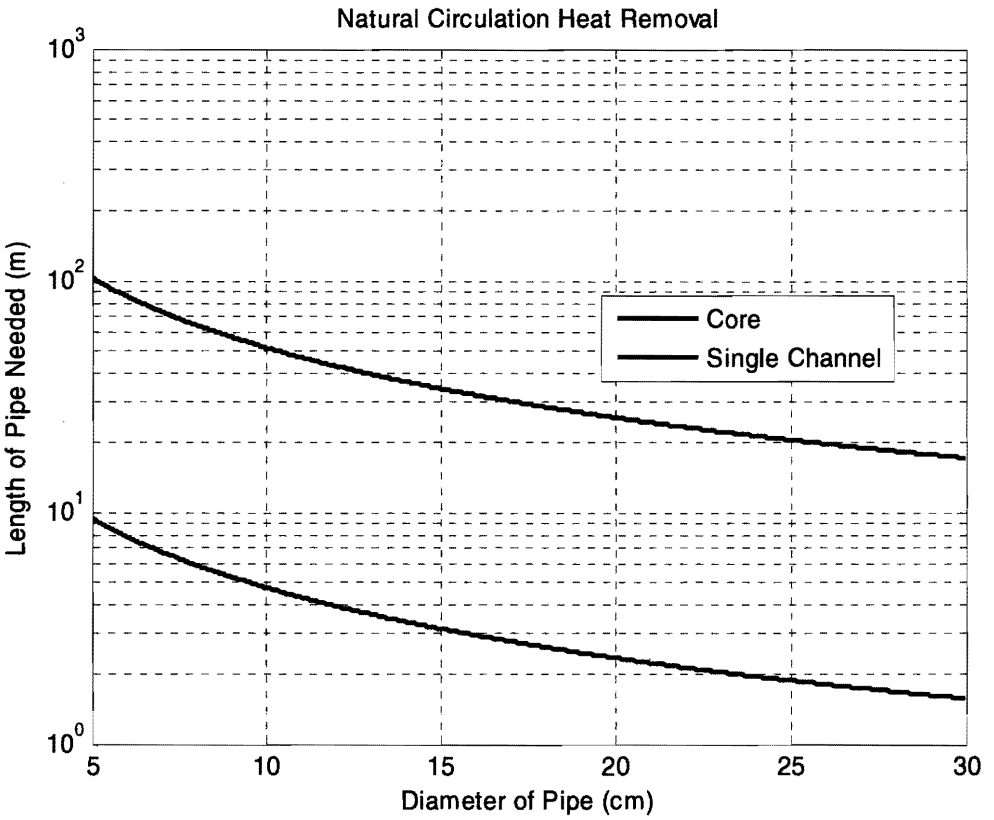

Figure 8: Plot of the maximum pipe length to allow natural circulation versus pipe diameter for several L/D values.

Secondary System

The secondary system for the project design is a helium-fed gas turbine operating on an idealized closed loop Brayton cycle. Much consideration and research has gone into this decision. This particular design proves to be the most promising for achieving the design criteria for the project.

When considering a secondary system for our remote reactor, two central options presented themselves. First considered for the project was the traditional steam turbine system. This system has the benefits of being widely used and understood in the majority

of modern nuclear power plants. In addition, because of this, one could easily obtain a stock system and quickly incorporate it into the reactor design. However, a steam turbine system also presented several flaws concerning our design criteria. The large weight of the necessary steam generators opposed attempts to maintain a light, highly transportable overall system. High maintenance requirements of this apparatus also caused mild concern, as the reactor should conceivably be useable in an area where this is the primary source of electricity and thus is designed to have as little down time as possible. Also since a second loop is already required to take care of the radiation transport problem of sodium, adding extra weight by requiring a pressure vessel would not be advantageous. Thus to optimize the transportation criteria of the design, the project does not incorporate a steam turbine, but instead utilizes a form of gas propelled turbine.

A gas turbine easily fulfills the minimum weight and complexity concerns by eliminating the need of pressure vessel and a steam generator. By circulating a chemically inert gas, through and intermediate loop, any contamination transfer between the primary and secondary loops will be eliminated. The compressible gas also does not need to be dried as does steam, thus eliminating the bulk of the steam driers and causing far less detrimental impact on the turbine itself. Less equipment allows for less malignance, more reliability, and more maintainability. Gas turbines do require higher temperatures in order to achieve an appreciable efficiency, but the reactor design should easily be able to meet this need. In addition, no current power plants operate a gas turbine in the recirculatory manner we propose. Additional research and development may need to be employed to determine the full feasibility and design elements of this type of system, but by operating on a closed loop Brayton cycle appreciable efficiencies could be achieved to meet the

100MWe goal. A typical large simple cycle gas turbine may produce 100 to 300 megawatts of power and have 35 to 40% thermal efficiency [4].

Ideal Brayton cycles operate by isentropically compressing air, then heating it to an expansion over the turbine until reverting to the initial pressure. In practice, general turbulence and frictional losses cause non-isentropic compression and expansion thus creating a need for higher delivery temperatures than the ideal model and means there is less available expansion to turn the generator. Despite these negatives, a gas turbine may still be successfully employed to create the needed power for our remote reactor system.

The project model for the secondary system is based on the Siemens Power SGT-800 Industrial Gas Turbine [4], seen in Figure 9. All calculations for the reactor have been made using certian assumptions made from the specifications of this turbine system. Each

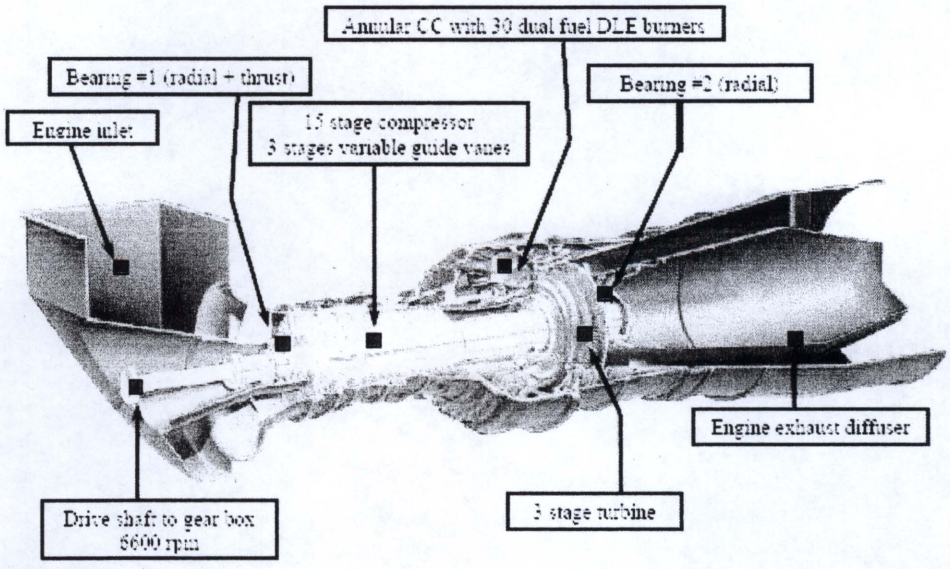

Figure 9: SGT-800 Industrial Gas Turbine – 45 MW

turbine is capable of outputting up to 45 MWe, so in order to achieve around 100 MWe output, two or three turbines will be set up in series. Two turbines could be used to get 90 MWe output, but if reliability is more important, it would be better to run three turbines below 100% capacity. The technical specifications for the SGT-800, listed in Table 9, are used as guideline for all calculated values and efficiencies [4]. In addition, the turbines will be modified for closed-cycle operation.

Table 9: SGT-800 Industrial Gas Turbine Technical Specifications

Technical specifications:	
Fuel	Natural gas
Frequency	50/60 Hz
Electrical output	45 MW in simple cycle 63.9 MW in combined cycle
Electrical efficiency	37% in simple cycle 54% in combined cycle
Heat rate	9,730 kJ/kWh (simple cycle)
Turbine speed	6,600 rpm
Compressor pressure ratio	19:1
Exhaust gas flow	130 kg/s
Exhaust gas temperature	538 deg C
NOx emissions (corr. to 15% O2, dry)	< 15 vppm

Overall secondary system efficiency is assumed to be 20% to compensate for losses across the heat exchanger. The secondary loop's efficiency can be improved by adding recouperators. If three turbines are used, each turbine will operate at approximately 33.3 MWe, which is well below their capacity. A full list of the assumed specifications for the project turbine system is listed in Table 10 below [4].

Table 10: Theoretical Closed Loop Gas Turbine Technical Specifications

Technical specifications:	
Frequency	50/60 Hz
Electrical output	45 MW in simple cycle
Electrical efficiency	20%
Turbine speed	6,600 rpm
Compressor pressure ratio	19:1
Exhaust gas flow	130 kg/s
Exhaust gas temperature	538 deg C
Circulated Gas	Helium

For the secondary system to operate on a closed loop Brayton cycle, helium will be first pumped through a compressor, then under pressure moved into a heat exchanger with the intermediate loop. From there the helium will be allowed to expand across the three serial turbines before being cooled, returning to its initial pressure, and being recirculated. This process can be viewed below in Figure 10.

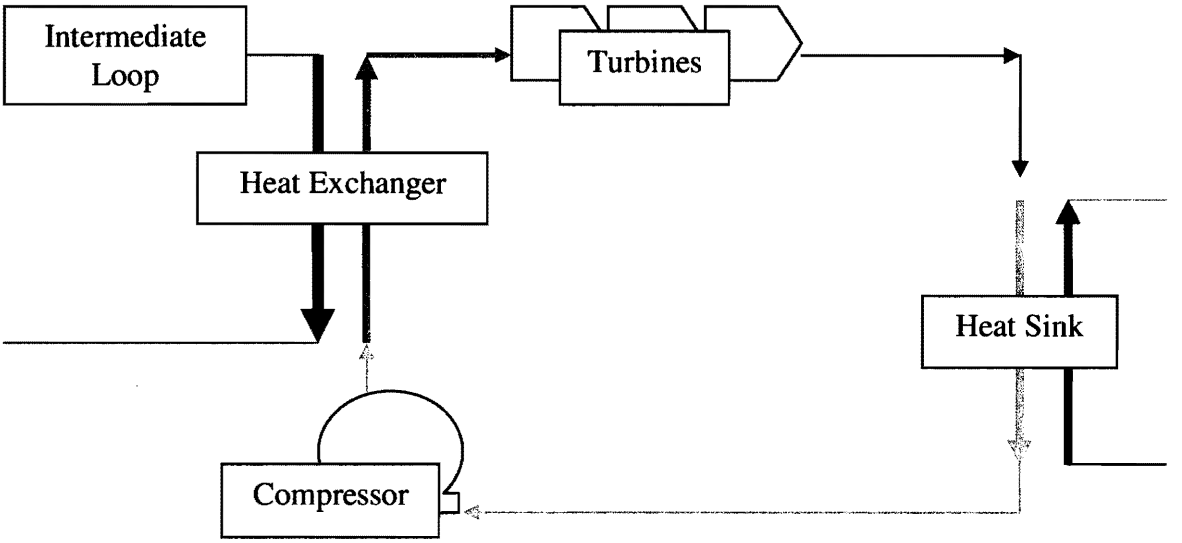

Figure 10: Closed Loop Brayton Cycle

Helium has been chosen both for its excellent thermal properties and low chemical reactivity as a noble gas. It's properties are listed below in Table 11.

Table 11: Properties of Helium

He Properties	
State	Gas
Thermal Conductivity	0.1513 W m^{-1} K^{-1}
Melting Point	0.95 K
$\Delta_f H°$	0 kJ mol^{-1}
$\Delta_f G°$	0 kJ mol^{-1}
S°	126.153 J K^{-1} mol^{-1}
$C_p H$	20.786 J K^{-1} mol^{-1}
Velocity of Sound	970 m s^{-1}

Safety

Shielding

Shielding a fast reactor can be very expensive and heavy. For a modular portable reactor, more site prep is required. To shield our reactor, we decided to utilize the ground. A hole will be dug into the ground and a concrete shell will be built on the inside of the hole to allow extra shielding, strength, and for keeping water from being contaminated. Next, the reactor will be inserted into the hole, leaving two meters of earth above the top of the reactor vessel.

With this site preparation in mind, SCALE was then again utilized to determine the necessary shielding required. Polyethylene was utilized to slow down neutrons and

stainless steel was used to shield against gammas. These two materials were alternated in layers of 5 to 10 cm for 22 layers (11 layers total of each material). Finally, a 31 cm layer of concrete was used. The total thickness of the shield came to 2.96 meters. The shield will be installed as a flat disk across the top of the opening. The operating room will be built over top of the two meters of concrete. A large, hydraulically operated arm has been envisioned for sliding the slab off the top of the hole for core replacement. An example of the conceptual design can be seen below in Figure 11.

Shielding during transportation was simple. The reactor core has not been started before, and thus the only fission occurring is due to spontaneous fission. The bare reactor core was determined via SCALE modeling to have a dose rate higher than 0.5 mrem/hr. A layer 5 inches thick of polyethylene easily reduced the limit set.

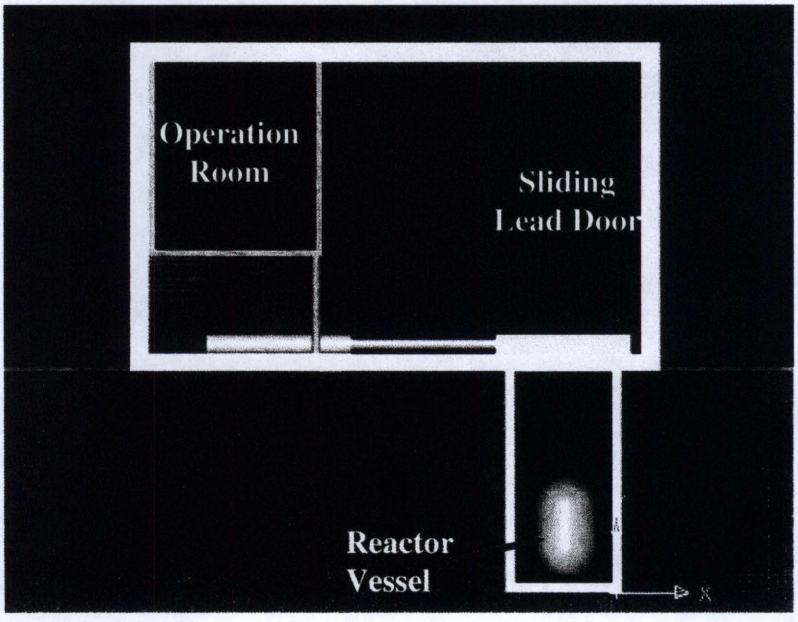

Figure 11: Visual representation of the reactor's shielding

Passive Safety System

Passive safety systems are ideal systems, as they require no input from an operator and are fail safe, meaning if they fail at all, they will fail in a way that will shut down the chain reaction. The most common and easy to implement passive safety system is control rod drive mechanisms (CRDMs) that insert into the core from the top and are magnetically connected to the control rods. This allows the control rods to drop freely under the force of gravity into the core should power delivered to the CRDMs be lost. Other passive safety systems include the negative temperature and void coefficients, as described above in the neutronics section of the report.

Loss of Coolant Accident

Although relatively little time exists for a full-blown accident analysis, a simplified Loss of Coolant Accident (LOCA) was analyzed. The analysis simply consisted of ensuring that the reactor could be safely shut down in the event of a sudden double-ended guillotine break in one of the main coolant lines. The simulation of this accident was accomplished by reducing the sodium density in the SCALE input deck to 0.0001 g/cm^3. The assumption in this analysis is that the control rods would immediately be fully inserted into the reactor the moment the double-ended guillotine break occurred and the sodium would be instantly evacuated from the reactor vessel. The SCALE input deck can be viewed in Appendix G and the K_{eff} of the SCALE output can be viewed in Table 12. A quick glimpse at the shut down column in this table reveals that the K_{eff} is less than one

for the entire life of the core. The output shows that a double-ended guillotine break is survivable.

Table 12: Determination of Safe Shutdown with a LOCA

K_{eff} for LOCA Shut Down		
Days	Normal	Shut Down
0	1.2683	0.8436
208	1.2641	0.9867
625	1.2557	0.9849
1042	1.2472	0.9828
1458	1.2387	0.9807
1875	1.2301	0.9786
2292	1.2214	0.9766
2708	1.2126	0.9745
3125	1.2038	0.9724
3542	1.1949	0.9703
3959	1.186	0.9683
4375	1.177	0.9662
4792	1.168	0.9641
5209	1.159	0.962
5625	1.1499	0.9599
6042	1.1409	0.9579
6459	1.1319	0.9558
6875	1.1229	0.9537
7292	1.114	0.9517
7709	1.1051	0.9496
8126	1.0963	0.9475
8542	1.0875	0.9455
8959	1.0789	0.9434
9376	1.0703	0.9413
9792	1.0619	0.9393

Loss of Flow Accident

Electromagnetic pumps are currently envisioned for this design. These pumps use electricity to create magnetic fields that will push the sodium coolant through the primary system. Loss of flow accidents occur when for some reason the coolant pumps fail. In case of a loss of flow accident, the reactor design has been designed so that natural

circulation occurs. Natural circulation will allow the coolant to sufficiently remove the decay heat after the core is shut down.

Other Design Criteria

Heat Sink

For a portable fast liquid metal cooled reactor, there are certain design criteria that need to be met. For any power cycle to work, there needs to be a heat sink. A basic shell and tube heat exchanger was selected to cool the sodium. This heat exchanger consists of the coolant loop flowing into many smaller pipes where a refrigerant or water flows across the small pipes, thus cooling the gas of the secondary, as seen in Figure 12.

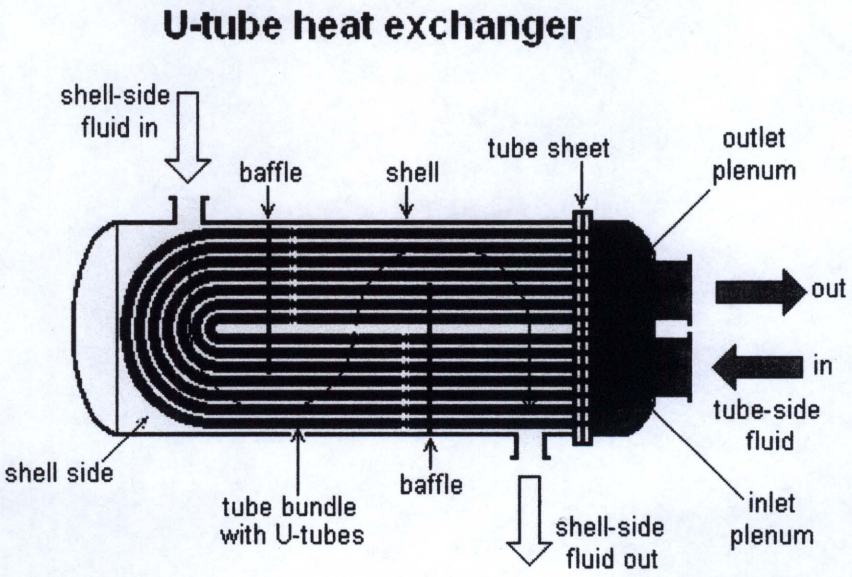

Figure 12: Basic Shell and Tube Heat Exchanger

Auxiliary Heaters

Due to the use of sodium as the reactor coolant, there are a couple extra parts needed. As previously discussed, the use of sodium requires an intermediate loop to be introduced to

the system to remove the risk of radioactive sodium getting in the secondary heat exchanger. In addition, since sodium is solid at room temperature, auxiliary heaters are required to startup the reactor. Coil heaters will be wrapped around the sodium pipes and turned on for startup.

Transportation

The weight of the reactor core is approximately 79.1 tons. This is too large for a normal tractor-trailer so therefore our reactor must be transported by a lowboy tractor-trailer. A lowboy is a special trailer that is ten feet wide and 40 to 60 feet long. These trailers are capable of hauling loads between 25 and 150 tons. A particular example of a lowboy is the 100-ton SP100L-5X ROGERS® lowboy. This lowboy, from Rogers Brothers Corporation out of Albion, Pennsylvania, is pictured below in Figure 13. This particular trailer is capable of handling our reactor core with capability to spare.

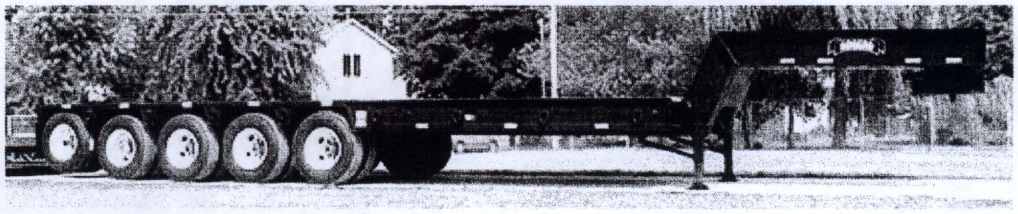

Figure 13: ROGERS® 100 Ton Lowboy

To split the design up into transportable sections, we will need one lowboy for the reactor vessel. Another three lowboys will be used to carry the gas turbines. The heat exchanger and pipes will go on a fifth truck. Pre-made slabs of shielding will be transported on a sixth truck and can be set into place by crane. The crane and an excavator will both need to be transported by lowboy as well for site preparation work. A tanker truck can be

utilized to transport the sodium coolant, provided an apparatus exists which can heat the sodium and pump it from the tanker truck and into the primary coolant system. Finally, depending on the location of the reactor, a number of truck based radiators will be necessary to cool the secondary. We decided to use a secondary system that avoided the problem of being dependent on a local supply of water to cool the reactor vessel. This will allow the system to be transported anywhere in the world where at least a dirt road exists.

A consideration of importance to a modular reactor during transportation is foreign material exclusion. A system of orifice covers needs to be implemented to prevent dirt, dust, or any other particles from fouling any of the equipment. This dirt and dust, if trapped within the system, can potentially degrade long term performance of the equipment and thus wear out before the lifetime of the core is expired.

Conclusions

Design of a modular, transportable reactor system is both feasible and practical, through the utilization of Liquid Metal Fast Breeder Reactor technology. A sodium cooled LMFBR is able to achieve the desired 100MWe output and also maintain all the transportability and safety design criteria associated with the small system reactor. By dividing the plant into small connecting subsystems, the components of the project can be pre-built and pre-loaded with fuel to be quickly assembled and put into service after transporting the system to any designated location.

The primary loop and reactor vessel will circulate the sodium coolant providing effective heat transfer to the secondary system. If presented with a loss of power circumstance resulting in a loss of pumping power, the sodium will provide natural circulation in order to maintain core temperature. Also in a Loss of Coolant Accident the negative void coefficient will lead to a natural reactor shutdown. The use of a sodium coolant lends many such desirable features to the design. Also due to sodium's lack of neutron moderation, fertile uranium isotopes can be converted into useable fuel.

A closed loop Brayton cycle is the basis of the gas turbine secondary system. By using a gas turbine instead of steam turbine the extra weight of a pressure vessel is not added. Also, adding in an intermediate loop eliminates the transfer of radioactive sodium from the primary loop to the secondary heat exchanger. Assuming 20% efficiency out of the secondary system, the primary reactor loop will have to operate at a 500 MWt power level. According to test codes evaluated using SCALE programs, this is readily achieved by our reactor setup. No commercially operated reactor currently uses a gas turbine system of this nature. Although the authors of this paper believe such a system could be adapted from current gas turbine designs, the authors also recommend further study into the feasibility and development of this system.

Fueling this reactor is 19% enriched uranium dioxide. By remaining under the 20% enrichment level, there is minimal proliferation risk during transport, yet there remains enough fertile material to prolong the fuel life to approximately 27 years without refueling. This allows for offsite refueling and upholds the long fuel cycle criteria of the

project. Standard stainless steel cladding and boron control rods along with the sodium coolant make up the rest of the core.

In order to shield both personnel and the environment from the radiation of the reactor, the reactor core and related systems are buried below two meters of earth and covered by a three meter thick layer of concrete and steel that includes a retractable lead door. This lowers the outside dose to an acceptable 0.46 mRem/hr, and protects the above systems and personnel while also adding an additional layer of protection from proliferation concerns.

Table 13: Reactor Parameters

Radius (m)	1.13
Diameter (m)	2.25
Height (m)	2.08
Fuel Pins	68589
Control Rods	4802
Total Pins and Rods	73391
radius fuel pellet (m)	2.90×10^{-3}
radial gap thickness (m)	1.20×10^{-4}
radial clad thickness (m)	3.80×10^{-4}
Core Thermal Power (MWth)	5.00×10^{8}
Heat Transfer (W/cm)	37
Core Volume (m^3)	8.31
Expected Core Lifetime (days)	10,000
Weight (tons)	76
Assumed Efficiency	20%
Assumed Electric Production (MWe)	100

From these results one can conclude that a basic modular LMFBR type reactor can be employed to fulfill all the requirements of this design project with the parameters designated in Table 13. While further research is recommended for the secondary system, safety analysis, auxiliary systems, and other areas, the authors believe that a viable design

can be fully developed from the preliminary work presented within this report. A 100MWe modular, transportable, rugged reactor system can be made and taken to remote locations.

Future work

While we feel our design is a competent, effective, and efficient one, there is still room for improvement as in all research projects. Some of the things we would most like to further investigate include fuel type, shape, and size, reactor shape, as well as coolant and shielding options.

The most important part of a reactor is the fuel. In our reactor, we are using small cylindrical pellets of Uranium oxide with 19% enrichment. There are four conditions which can all be changed to either increase or decrease output of power. To begin with, we will look at the type of fuel being used. We felt that Uranium dioxide is the best fuel because of high efficiency with low enrichment. Other possibilities we could look at would include plutonium oxide, uranium tetraflouride and a mixture of uranium and plutonium. All of these fuels would be efficient and produce the results we desire, but much research would be needed. The major setback would be the concerns of proliferation when using plutonium. This would cause more safeguards to be put in place to prevent any tampering or theft of the fuel.

In addition to changing the type of fuel used, we can also consider the size and shape of the fuel. Our original design included fuel plates. We still feel this is and adequate design that would not only produce the required results but also be a unique design. The

biggest problem is the amount of effort required to do thermal analysis for this type of fuel. This again is able to be done, but requires more time than we have. If we are able to change the shape of the fuel, one would believe that we could also change the size of the fuel. The fuel pellets being used are very small but efficient. There is a good possibility that with more time, we could find a way to use larger fuel pellets to increase initial as well as long term power output.

We see there are several avenues of possible improvement for the fuel, but what about the structure that contains the fuel. Cylindrical reactors have been used for years and are heavily favored in most design aspects. That does not mean though that other shapes of reactors could not be used. We originally felt a spherical reactor would be a unique design that could give us our desired output. Though we were able to find a spherical reactor to work for our neutronic calculations, we would have faced many problems on the thermal analysis of it. Once again we feel that with more time, we would be able to make this design work properly and possibly even give us a higher efficiency output than a spherical reactor.

Sodium coolant has been shown to work well as the main coolant in our design as well as other designs. We still feel that with the proper resources, we would be able to use mercury as our coolant and actually be happier with the results.

Finally, we looked at shielding. Concrete and lead are a great source of shielding largely because of high density and large capture cross sections. The containment structure we have designed will shield well enough to allow workers to be present during operation.

Some other avenues we could possibly consider for our shielding would include burying the reactor further into the ground, or using possibly using a metal/U-238 mixture for the containment. All of these materials will shield against the particles that cause us harm, but require more research.

References

[1]. Carlsson, Johan & Wider, Hartmut. "Comparison of sodium and lead-coold fast reactors regarding reactor physics aspects, sever safety and economical issues." Joint Research Centre of the European Commission, Institue of Energy. April 2006.

[2]. Duderstadt, James J., and Louis J. Hamilton. *Nuclear Reactor Analysis*. Canada: John Wiley & Sons, Inc., 1976.

[3]. E. T. Jurney, Jane H. Hall, David B. Hall, Avery M. Gage, Nat H. Godbold, Arthur R. Sayer, and Earl O. Swickard, "The Los Alamos Fast Plutonium Reactor," Los Alamos Scientific Laboratory reportLA-1679 (1954).

[4]. Hagerstål, Thomas, and Jan Wikner. "Development &Operating Experience with SGT-800 a Siemens 45 MW Industrial Gas Turbine for Various Applications." 6th Annual Australian Gas Turbines Conference. Brisbane, Australia, 2005.

[5] Holden, Brandon. "Program to calculate various heat transfer activities in a liquid metal cooled modular fast reactor." 2007.

[6]. Michal, Rick. "Fifty years ago in December: Atomic reactor EBR-I produced first electricity." American Nuclear Society Newsletter. November 2001 pg 28-29.

[7]. Simna, Massoud T. "Fuel Element Experience in Nuclear Power Reactors." Gordon and Breach Publishing, Ic., 2006

[8]. Matzke, Hj. "Science of Advanced LMFBR Fuels: A Monograph on Solid State Physics, Chemistry and Technology of Carbides, Nitrides and Carbonitrides of Uranium and Plutonium." North Holland, Amsterdam, 1986.

[9]. Shultis, Kenneth J., and Richard E. Faw. *Radiation Shielding*. La Grange Park, Illinois 60526 USA: American Nuclear Society, Inc., 1996.

[10]. Todreas, Neil E., and Mujid S. Kazimi. *Nuclear Systems I: Thermal Hydraulic Fundamentals*. New York, NY 10016: Taylor & Francis Group, 1990.

Appendix A: Normal Operating SCALE Input Deck

```
=sas2h      parm='skipshipdata
'************************************************
'   LMFBR from Duderstadt & Hamilton App. H.
'************************************************
LMFBR
44groupndf5          Latticecell
uo2       1  1.0  2800 92235 19 92238 81 end
ss316     2  1.0  1563.15 end
na        3  den=0.927 1.0  739.15  end
ag-109     1  1.e-20 2300 end
ag-111     1  1.e-20 2300 end
ba-138     1  1.e-20 2300 end
br-81      1  1.e-20 2300 end
ce-140     1  1.e-20 2300 end
ce-141     1  1.e-20 2300 end
ce-142     1  1.e-20 2300 end
ce-143     1  1.e-20 2300 end
ce-144     1  1.e-20 2300 end
cs-133     1  1.e-20 2300 end
cs-135     1  1.e-20 2300 end
cs-136     1  1.e-20 2300 end
cs-137     1  1.e-20 2300 end
eu-153     1  1.e-20 2300 end
eu-155     1  1.e-20 2300 end
eu-156     1  1.e-20 2300 end
i-127      1  1.e-20 2300 end
i-129      1  1.e-20 2300 end
i-131      1  1.e-20 2300 end
kr-83      1  1.e-20 2300 end
kr-84      1  1.e-20 2300 end
kr-85      1  1.e-20 2300 end
kr-86      1  1.e-20 2300 end
la-139     1  1.e-20 2300 end
la-140     1  1.e-20 2300 end
mo-95      1  1.e-20 2300 end
mo-97      1  1.e-20 2300 end
mo-98      1  1.e-20 2300 end
mo-99      1  1.e-20 2300 end
mo-100     1  1.e-20 2300 end
nb-95      1  1.e-20 2300 end
nd-143     1  1.e-20 2300 end
nd-144     1  1.e-20 2300 end
nd-145     1  1.e-20 2300 end
nd-146     1  1.e-20 2300 end
nd-147     1  1.e-20 2300 end
nd-148     1  1.e-20 2300 end
nd-150     1  1.e-20 2300 end
pd-105     1  1.e-20 2300 end
pd-107     1  1.e-20 2300 end
pd-108     1  1.e-20 2300 end
pm-147     1  1.e-20 2300 end
pm-148     1  1.e-20 2300 end
pr-141     1  1.e-20 2300 end
pr-143     1  1.e-20 2300 end
rb-85      1  1.e-20 2300 end
rh-103     1  1.e-20 2300 end
ru-101     1  1.e-20 2300 end
ru-102     1  1.e-20 2300 end
ru-103     1  1.e-20 2300 end
ru-104     1  1.e-20 2300 end
ru-106     1  1.e-20 2300 end
sb-125     1  1.e-20 2300 end
sb-126     1  1.e-20 2300 end
se-80      1  1.e-20 2300 end
se-82      1  1.e-20 2300 end
sm-149     1  1.e-20 2300 end
sm-151     1  1.e-20 2300 end
sm-152     1  1.e-20 2300 end
```

```
sm-154    1  1.e-20 2300 end
sn-125    1  1.e-20 2300 end
sn-126    1  1.e-20 2300 end
sr-88     1  1.e-20 2300 end
sr-89     1  1.e-20 2300 end
sr-90     1  1.e-20 2300 end
tc-99     1  1.e-20 2300 end
te-128    1  1.e-20 2300 end
te-130    1  1.e-20 2300 end
te-132    1  1.e-20 2300 end
xe-131    1  1.e-20 2300 end
xe-132    1  1.e-20 2300 end
xe-133    1  1.e-20 2300 end
xe-134    1  1.e-20 2300 end
xe-135    1  1.e-20 2300 end
xe-136    1  1.e-20 2300 end
y-89      1  1.e-20 2300 end
y-91      1  1.e-20 2300 end
zr-91     1  1.e-20 2300 end
zr-92     1  1.e-20 2300 end
zr-93     1  1.e-20 2300 end
zr-94     1  1.e-20 2300 end
zr-95     1  1.e-20 2300 end
zr-96     1  1.e-20 2300 end
end comp
squarepitch 0.7374 .58  1  3  .68 2  .604  3  end
NPIN/ASSM=68589 FUELNGTH=208.28 NCYCLES=1 NLIB/CYC=24
 PRINTLEVEL=4 INPLEVEL=3 NUMZTOTAL=4  end
3 0.001 500 98.87 2 106.49 3 199
BON end
NIT end
XSD
Weighted cross sections
I4= -1 3 0 9
X5= .0001 .00001 1. 0. 0. 1.42 182.88 end
POWER=500. BURN=9999 DOWN=15 end
end
```

Appendix B: Void Coefficient Determination SCALE Input Deck

```
=sas2h      parm='skipshipdata
'************************************************
'   LMFBR from Duderstadt & Hamilton App. H.
'************************************************
LMFBR
44groupndf5          Latticecell
uo2       1  1.0  2800 92235 19 92238 81 end
ss316     2  1.0  1563.15 end
na        3  den=0.500 1.0  739.15  end
ag-109    1  1.e-20 2300 end
ag-111    1  1.e-20 2300 end
ba-138    1  1.e-20 2300 end
br-81     1  1.e-20 2300 end
ce-140    1  1.e-20 2300 end
ce-141    1  1.e-20 2300 end
ce-142    1  1.e-20 2300 end
ce-143    1  1.e-20 2300 end
ce-144    1  1.e-20 2300 end
cs-133    1  1.e-20 2300 end
cs-135    1  1.e-20 2300 end
cs-136    1  1.e-20 2300 end
cs-137    1  1.e-20 2300 end
eu-153    1  1.e-20 2300 end
eu-155    1  1.e-20 2300 end
eu-156    1  1.e-20 2300 end
i-127     1  1.e-20 2300 end
i-129     1  1.e-20 2300 end
i-131     1  1.e-20 2300 end
kr-83     1  1.e-20 2300 end
kr-84     1  1.e-20 2300 end
kr-85     1  1.e-20 2300 end
kr-86     1  1.e-20 2300 end
la-139    1  1.e-20 2300 end
la-140    1  1.e-20 2300 end
mo-95     1  1.e-20 2300 end
mo-97     1  1.e-20 2300 end
mo-98     1  1.e-20 2300 end
mo-99     1  1.e-20 2300 end
mo-100    1  1.e-20 2300 end
nb-95     1  1.e-20 2300 end
nd-143    1  1.e-20 2300 end
nd-144    1  1.e-20 2300 end
nd-145    1  1.e-20 2300 end
nd-146    1  1.e-20 2300 end
nd-147    1  1.e-20 2300 end
nd-148    1  1.e-20 2300 end
nd-150    1  1.e-20 2300 end
pd-105    1  1.e-20 2300 end
pd-107    1  1.e-20 2300 end
pd-108    1  1.e-20 2300 end
pm-147    1  1.e-20 2300 end
pm-148    1  1.e-20 2300 end
pr-141    1  1.e-20 2300 end
pr-143    1  1.e-20 2300 end
rb-85     1  1.e-20 2300 end
rh-103    1  1.e-20 2300 end
ru-101    1  1.e-20 2300 end
ru-102    1  1.e-20 2300 end
ru-103    1  1.e-20 2300 end
ru-104    1  1.e-20 2300 end
ru-106    1  1.e-20 2300 end
sb-125    1  1.e-20 2300 end
sb-126    1  1.e-20 2300 end
se-80     1  1.e-20 2300 end
se-82     1  1.e-20 2300 end
sm-149    1  1.e-20 2300 end
sm-151    1  1.e-20 2300 end
sm-152    1  1.e-20 2300 end
```

```
sm-154    1  1.e-20 2300 end
sn-125    1  1.e-20 2300 end
sn-126    1  1.e-20 2300 end
sr-88     1  1.e-20 2300 end
sr-89     1  1.e-20 2300 end
sr-90     1  1.e-20 2300 end
tc-99     1  1.e-20 2300 end
te-128    1  1.e-20 2300 end
te-130    1  1.e-20 2300 end
te-132    1  1.e-20 2300 end
xe-131    1  1.e-20 2300 end
xe-132    1  1.e-20 2300 end
xe-133    1  1.e-20 2300 end
xe-134    1  1.e-20 2300 end
xe-135    1  1.e-20 2300 end
xe-136    1  1.e-20 2300 end
y-89      1  1.e-20 2300 end
y-91      1  1.e-20 2300 end
zr-91     1  1.e-20 2300 end
zr-92     1  1.e-20 2300 end
zr-93     1  1.e-20 2300 end
zr-94     1  1.e-20 2300 end
zr-95     1  1.e-20 2300 end
zr-96     1  1.e-20 2300 end
end comp
squarepitch 0.7374 .58  1  3  .68 2  .604  3  end
NPIN/ASSM=68589 FUELNGTH=208.28 NCYCLES=1 NLIB/CYC=24
  PRINTLEVEL=4 INPLEVEL=3 NUMZTOTAL=4  end
3 0.001 500 98.87 2 106.49 3 199
BON end
NIT end
XSD
Weighted cross sections
I4= -1 3 0 9
X5= .0001 .00001 1. 0. 0. 1.42 182.88 end
POWER=500. BURN=9999 DOWN=15 end
end
```

Appendix C: Temperature Coefficient Determination SCALE Input Deck

```
=sas2h      parm='skipshipdata
'************************************************
'   LMFBR from Duderstadt & Hamilton App. H.
'************************************************
LMFBR
44groupndf5          Latticecell
uo2       1  1.0  2300 92235 19 92238 81 end
ss316     2  1.0  1200 end
na        3  den=0.927 1.0  739.15  end
ag-109    1  1.e-20 2300 end
ag-111    1  1.e-20 2300 end
ba-138    1  1.e-20 2300 end
br-81     1  1.e-20 2300 end
ce-140    1  1.e-20 2300 end
ce-141    1  1.e-20 2300 end
ce-142    1  1.e-20 2300 end
ce-143    1  1.e-20 2300 end
ce-144    1  1.e-20 2300 end
cs-133    1  1.e-20 2300 end
cs-135    1  1.e-20 2300 end
cs-136    1  1.e-20 2300 end
cs-137    1  1.e-20 2300 end
eu-153    1  1.e-20 2300 end
eu-155    1  1.e-20 2300 end
eu-156    1  1.e-20 2300 end
i-127     1  1.e-20 2300 end
i-129     1  1.e-20 2300 end
i-131     1  1.e-20 2300 end
kr-83     1  1.e-20 2300 end
kr-84     1  1.e-20 2300 end
kr-85     1  1.e-20 2300 end
kr-86     1  1.e-20 2300 end
la-139    1  1.e-20 2300 end
la-140    1  1.e-20 2300 end
mo-95     1  1.e-20 2300 end
mo-97     1  1.e-20 2300 end
mo-98     1  1.e-20 2300 end
mo-99     1  1.e-20 2300 end
mo-100    1  1.e-20 2300 end
nb-95     1  1.e-20 2300 end
nd-143    1  1.e-20 2300 end
nd-144    1  1.e-20 2300 end
nd-145    1  1.e-20 2300 end
nd-146    1  1.e-20 2300 end
nd-147    1  1.e-20 2300 end
nd-148    1  1.e-20 2300 end
nd-150    1  1.e-20 2300 end
pd-105    1  1.e-20 2300 end
pd-107    1  1.e-20 2300 end
pd-108    1  1.e-20 2300 end
pm-147    1  1.e-20 2300 end
pm-148    1  1.e-20 2300 end
pr-141    1  1.e-20 2300 end
pr-143    1  1.e-20 2300 end
rb-85     1  1.e-20 2300 end
rh-103    1  1.e-20 2300 end
ru-101    1  1.e-20 2300 end
ru-102    1  1.e-20 2300 end
ru-103    1  1.e-20 2300 end
ru-104    1  1.e-20 2300 end
ru-106    1  1.e-20 2300 end
sb-125    1  1.e-20 2300 end
sb-126    1  1.e-20 2300 end
se-80     1  1.e-20 2300 end
se-82     1  1.e-20 2300 end
sm-149    1  1.e-20 2300 end
sm-151    1  1.e-20 2300 end
sm-152    1  1.e-20 2300 end
```

```
sm-154    1  1.e-20 2300 end
sn-125    1  1.e-20 2300 end
sn-126    1  1.e-20 2300 end
sr-88     1  1.e-20 2300 end
sr-89     1  1.e-20 2300 end
sr-90     1  1.e-20 2300 end
tc-99     1  1.e-20 2300 end
te-128    1  1.e-20 2300 end
te-130    1  1.e-20 2300 end
te-132    1  1.e-20 2300 end
xe-131    1  1.e-20 2300 end
xe-132    1  1.e-20 2300 end
xe-133    1  1.e-20 2300 end
xe-134    1  1.e-20 2300 end
xe-135    1  1.e-20 2300 end
xe-136    1  1.e-20 2300 end
y-89      1  1.e-20 2300 end
y-91      1  1.e-20 2300 end
zr-91     1  1.e-20 2300 end
zr-92     1  1.e-20 2300 end
zr-93     1  1.e-20 2300 end
zr-94     1  1.e-20 2300 end
zr-95     1  1.e-20 2300 end
zr-96     1  1.e-20 2300 end
end comp
squarepitch 0.7374 .58  1  3  .68 2  .604  3  end
NPIN/ASSM=68589 FUELNGTH=208.28 NCYCLES=1 NLIB/CYC=24
  PRINTLEVEL=4 INPLEVEL=3 NUMZTOTAL=4  end
3 0.001 500 98.87 2 106.49 3 199
BON end
NIT end
XSD
Weighted cross sections
I4= -1 3 0 9
X5= .0001 .00001 1. 0. 0. 1.42 182.88 end
POWER=500. BURN=9999 DOWN=15 end
end
```

Appendix D: Ensuring Shut-down Capability of Reactor SCALE Input Deck

```
=sas2h      parm='skipshipdata
'************************************************
'   LMFBR from Duderstadt & Hamilton App. H.
'************************************************
LMFBR
44groupndf5          Latticecell
uo2       1  0.9346  2800 92235 19 92238 81 end
boron     1  0.0654 1563.15 5010 30 5011 70 end
ss316     2  1.0  1563.15 end
na        3  den=0.927 1.0  739.15  end
ag-109    1  1.e-20 2300 end
ag-111    1  1.e-20 2300 end
ba-138    1  1.e-20 2300 end
br-81     1  1.e-20 2300 end
ce-140    1  1.e-20 2300 end
ce-141    1  1.e-20 2300 end
ce-142    1  1.e-20 2300 end
ce-143    1  1.e-20 2300 end
ce-144    1  1.e-20 2300 end
cs-133    1  1.e-20 2300 end
cs-135    1  1.e-20 2300 end
cs-136    1  1.e-20 2300 end
cs-137    1  1.e-20 2300 end
eu-153    1  1.e-20 2300 end
eu-155    1  1.e-20 2300 end
eu-156    1  1.e-20 2300 end
i-127     1  1.e-20 2300 end
i-129     1  1.e-20 2300 end
i-131     1  1.e-20 2300 end
kr-83     1  1.e-20 2300 end
kr-84     1  1.e-20 2300 end
kr-85     1  1.e-20 2300 end
kr-86     1  1.e-20 2300 end
la-139    1  1.e-20 2300 end
la-140    1  1.e-20 2300 end
mo-95     1  1.e-20 2300 end
mo-97     1  1.e-20 2300 end
mo-98     1  1.e-20 2300 end
mo-99     1  1.e-20 2300 end
mo-100    1  1.e-20 2300 end
nb-95     1  1.e-20 2300 end
nd-143    1  1.e-20 2300 end
nd-144    1  1.e-20 2300 end
nd-145    1  1.e-20 2300 end
nd-146    1  1.e-20 2300 end
nd-147    1  1.e-20 2300 end
nd-148    1  1.e-20 2300 end
nd-150    1  1.e-20 2300 end
pd-105    1  1.e-20 2300 end
pd-107    1  1.e-20 2300 end
pd-108    1  1.e-20 2300 end
pm-147    1  1.e-20 2300 end
pm-148    1  1.e-20 2300 end
pr-141    1  1.e-20 2300 end
pr-143    1  1.e-20 2300 end
rb-85     1  1.e-20 2300 end
rh-103    1  1.e-20 2300 end
ru-101    1  1.e-20 2300 end
ru-102    1  1.e-20 2300 end
ru-103    1  1.e-20 2300 end
ru-104    1  1.e-20 2300 end
ru-106    1  1.e-20 2300 end
sb-125    1  1.e-20 2300 end
sb-126    1  1.e-20 2300 end
se-80     1  1.e-20 2300 end
se-82     1  1.e-20 2300 end
sm-149    1  1.e-20 2300 end
sm-151    1  1.e-20 2300 end
```

```
sm-152    1  1.e-20 2300 end
sm-154    1  1.e-20 2300 end
sn-125    1  1.e-20 2300 end
sn-126    1  1.e-20 2300 end
sr-88     1  1.e-20 2300 end
sr-89     1  1.e-20 2300 end
sr-90     1  1.e-20 2300 end
tc-99     1  1.e-20 2300 end
te-128    1  1.e-20 2300 end
te-130    1  1.e-20 2300 end
te-132    1  1.e-20 2300 end
xe-131    1  1.e-20 2300 end
xe-132    1  1.e-20 2300 end
xe-133    1  1.e-20 2300 end
xe-134    1  1.e-20 2300 end
xe-135    1  1.e-20 2300 end
xe-136    1  1.e-20 2300 end
y-89      1  1.e-20 2300 end
y-91      1  1.e-20 2300 end
zr-91     1  1.e-20 2300 end
zr-92     1  1.e-20 2300 end
zr-93     1  1.e-20 2300 end
zr-94     1  1.e-20 2300 end
zr-95     1  1.e-20 2300 end
zr-96     1  1.e-20 2300 end
end comp
squarepitch 0.7374 .58  1  3  .68 2  .604  3  end
NPIN/ASSM=73391 FUELNGTH=208.28 NCYCLES=1 NLIB/CYC=24
 PRINTLEVEL=4 INPLEVEL=3 NUMZTOTAL=4  end
3 0.001 500 98.87 2 106.49 3 199
BON end
NIT end
XSD
Weighted cross sections
I4= -1 3 0 9
X5= .0001 .00001 1. 0. 0. 1.42 182.88 end
POWER=500. BURN=9999 DOWN=15 end
end
```

Appendix E: Normal Operating Dose Calculation SCALE Input Deck

```
#sas1x          parm='size=900000'
spherical reactor with concrete shielding
27n-18couple multiregion
'
' multiregion must be specified to run combined criticality/shielding problem.
'
uo2         1 0.4541 2800 92235 19 92238 81 end
ss316           1 0.1409 1563.15 end
na          1 0.3732 739.15 end
poly(h2o)    2 1.0 end
rfconcrete   3 1.0 end
ss316           4 1.0 end
activities   4 0  1.e-24 end
end comp
'
' the criticality calculation input
'
spherical vacuum end
1 134.5
end zone
' isn=16 is specified to match the angular quadrature in the shielding calc.
more data isn=16 end more data
end
last
reactor shielding
'
' the shielding calculation input
'
spherical
' first mixture must be void of 1 interval with outer dimension that matches
' outer dimension of shielding calculation.
' flags indicate boundary source will be input from xsdrnpm criticality calc.
0 134.5   1 1 0 0 0
4 142.12 100 0
2 149.5 100 0
4 154.5 100 0
2 159.5 100 0
4 164.5 100 0
2 169.5 100 0
4 174.5 100 0
2 179.5 100 0
4 184.5 100 0
2 189.5 100 0
4 194.5 100 0
2 199.5 100 0
4 204.5 100 0
2 209.5 100 0
4 214.5 100 0
2 219.5 100 0
4 224.5 100 0
2 229.5 100 0
4 244.5 100 0
4 384.5 100 0
2 389.5 100 0
4 399.5 100 0
3 430.5 100 0
end zone
read xsdose
end
```

Appendix F: Transportation Dose Calculation SCALE Input Deck

```
#sas1x          parm='size=900000'
spherical reactor with concrete shielding
27n-18couple multiregion
'
' multiregion must be specified to run combined criticality/shielding problem.
'
uo2         1 0.4541 2800 92235 19 92238 81 end
ss316           1 0.1409 1563.15 end
H2O         1 0.3732 739.150 end
boron       1 0.0318 1563.15  5010 30 5011 70 end
poly(h2o)    2 1.00 end
rfconcrete   3 0.99 end
B-10            3 0.01 end
ss316           4 1.00 end
activities   4 0  1.e-24 end
end comp
'
' the criticality calculation input
'
spherical vacuum end
1 134.5
end zone
' isn=16 is specified to match the angular quadrature in the shielding calc.
more data isn=16 end more data
end
last
reactor shielding
'
' the shielding calculation input
'
spherical
' first mixture must be void of 1 interval with outer dimension that matches
' outer dimension of shielding calculation.
' flags indicate boundary source will be input from xsdrnpm criticality calc.
0 134.5   1 1 0 0 0
4 142.12 2000 0
2 155.00 2000
end zone
read xsdose
end
```

Appendix G: LOCA Analysis SCALE Input Deck

```
=sas2h      parm='skipshipdata
'************************************************
'   LMFBR from Duderstadt & Hamilton App. H.
'************************************************
LMFBR
44groupndf5          Latticecell
uo2       1  0.9346  2800 92235 19 92238 81 end
boron     1  0.0654 1563.15 5010 36 5011 64 end
ss316     2  1.0  1563.15 end
na        3  den=0.0001 1.0  739.15  end
ag-109    1  1.e-20 2300 end
ag-111    1  1.e-20 2300 end
ba-138    1  1.e-20 2300 end
br-81     1  1.e-20 2300 end
ce-140    1  1.e-20 2300 end
ce-141    1  1.e-20 2300 end
ce-142    1  1.e-20 2300 end
ce-143    1  1.e-20 2300 end
ce-144    1  1.e-20 2300 end
cs-133    1  1.e-20 2300 end
cs-135    1  1.e-20 2300 end
cs-136    1  1.e-20 2300 end
cs-137    1  1.e-20 2300 end
eu-153    1  1.e-20 2300 end
eu-155    1  1.e-20 2300 end
eu-156    1  1.e-20 2300 end
i-127     1  1.e-20 2300 end
i-129     1  1.e-20 2300 end
i-131     1  1.e-20 2300 end
kr-83     1  1.e-20 2300 end
kr-84     1  1.e-20 2300 end
kr-85     1  1.e-20 2300 end
kr-86     1  1.e-20 2300 end
la-139    1  1.e-20 2300 end
la-140    1  1.e-20 2300 end
mo-95     1  1.e-20 2300 end
mo-97     1  1.e-20 2300 end
mo-98     1  1.e-20 2300 end
mo-99     1  1.e-20 2300 end
mo-100    1  1.e-20 2300 end
nb-95     1  1.e-20 2300 end
nd-143    1  1.e-20 2300 end
nd-144    1  1.e-20 2300 end
nd-145    1  1.e-20 2300 end
nd-146    1  1.e-20 2300 end
nd-147    1  1.e-20 2300 end
nd-148    1  1.e-20 2300 end
nd-150    1  1.e-20 2300 end
pd-105    1  1.e-20 2300 end
pd-107    1  1.e-20 2300 end
pd-108    1  1.e-20 2300 end
pm-147    1  1.e-20 2300 end
pm-148    1  1.e-20 2300 end
pr-141    1  1.e-20 2300 end
pr-143    1  1.e-20 2300 end
rb-85     1  1.e-20 2300 end
rh-103    1  1.e-20 2300 end
ru-101    1  1.e-20 2300 end
ru-102    1  1.e-20 2300 end
ru-103    1  1.e-20 2300 end
ru-104    1  1.e-20 2300 end
ru-106    1  1.e-20 2300 end
sb-125    1  1.e-20 2300 end
sb-126    1  1.e-20 2300 end
se-80     1  1.e-20 2300 end
se-82     1  1.e-20 2300 end
sm-149    1  1.e-20 2300 end
sm-151    1  1.e-20 2300 end
```

```
sm-152    1  1.e-20 2300 end
sm-154    1  1.e-20 2300 end
sn-125    1  1.e-20 2300 end
sn-126    1  1.e-20 2300 end
sr-88     1  1.e-20 2300 end
sr-89     1  1.e-20 2300 end
sr-90     1  1.e-20 2300 end
tc-99     1  1.e-20 2300 end
te-128    1  1.e-20 2300 end
te-130    1  1.e-20 2300 end
te-132    1  1.e-20 2300 end
xe-131    1  1.e-20 2300 end
xe-132    1  1.e-20 2300 end
xe-133    1  1.e-20 2300 end
xe-134    1  1.e-20 2300 end
xe-135    1  1.e-20 2300 end
xe-136    1  1.e-20 2300 end
y-89      1  1.e-20 2300 end
y-91      1  1.e-20 2300 end
zr-91     1  1.e-20 2300 end
zr-92     1  1.e-20 2300 end
zr-93     1  1.e-20 2300 end
zr-94     1  1.e-20 2300 end
zr-95     1  1.e-20 2300 end
zr-96     1  1.e-20 2300 end
end comp
squarepitch 0.7374 .58  1  3  .68 2  .604  3  end
NPIN/ASSM=73391 FUELNGTH=208.28 NCYCLES=1 NLIB/CYC=24
 PRINTLEVEL=4 INPLEVEL=3 NUMZTOTAL=4  end
3 0.001 500 98.87 2 106.49 3 199
BON end
NIT end
XSD
Weighted cross sections
I4= -1 3 0 9
X5= .0001 .00001 1. 0. 0. 1.42 182.88 end
POWER=500. BURN=9999 DOWN=15 end
end
```

Appendix H: Heat Transfer MatLab Code

```
%%%%%%%%%%%%%%%%%%%%%%%%%%%%%%%%%%%%%%%%%%%%%%%%%%%%%%%%%%%%%%%%%%%%%%%%%%%%%%%%%%%%%%%%%%%%%%%%%%%%%%%%%%%%%%%%%%%%%%%%%%%%%%%%%%%%%%%%%%%%%%%%%%%%%%%%%%%%%%%%%%%%%%%%%%%%%%%%%%%%%%%%%%%%%%%%%%%%%%%%%%%%%%%%%%%%%%%%%%%%%%%%%%%%%%%
%%%%%%%%%%%%%%%%%%%%%%%%
%Stuart Walker Sp. '07
%Senior Design NE 472
%Thermal Analysis of Portable Liquid Metal Cooled Fast Reactor
%%%%%%%%%%%%%%%%%%%%%%%%%%%%%%%%%%%%%%%%%%%%%%%%%%%%%%%%%%%%%%%%%%%%%%%%%%%%%%%%%%%%%%%%%%%%%%%%%%%%%%%%%%%%%%%%%%%%%%%%%%%%%%%%%%%%%%%%%%%%%%%%%%%%%%%%%%%%%%%%%%%%%%%%%%%%%%%%%%%%%%%%%%%%%%%%%%%%%%%%%%%%%%%%%%%%%%%%%%%%%%%%%%%%%%%
%%%%%%%%%%%%%%%%%%%%%%%%
clc
clear all

%%%%%%%%%%%%%%%%%%%%%%%%%%%%%%%%%%%%%%%%%%%%%%%%%%%%%%%%%%%%%%%%%%%%%%%%%%%%%%%%%%%%%%%%%%%%%%%%%%%%%%%%%%%%%%%%%%%%%%%%%%%%%%%%%%%%%%%%%%%%%%%%%%%%%%%%%%%%%%%%%%%%%%%%%%%%%%%%%%%%%%%%%%%%%%%%%%%%%%%%%%%%%%%%%%%%%%%%%%%%%%%%%%%%%%%
%%%%%%%%%%%%%%%%%%%%%%%%
%Parameters (SI)
%%%%%%%%%%%%%%%%%%%%%%%%%%%%%%%%%%%%%%%%%%%%%%%%%%%%%%%%%%%%%%%%%%%%%%%%%%%%%%%%%%%%%%%%%%%%%%%%%%%%%%%%%%%%%%%%%%%%%%%%%%%%%%%%%%%%%%%%%%%%%%%%%%%%%%%%%%%%%%%%%%%%%%%%%%%%%%%%%%%%%%%%%%%%%%%%%%%%%%%%%%%%%%%%%%%%%%%%%%%%%%%%%%%%%%%
%%%%%%%%%%%%%%%%%%%%%%%%%%

%Physical Constants
g = 9.8;
k_f = 3.6;
k_c = 62;
h_g = 5.7e3; %Todreas Ex 13-2
c_p_cool = 1300; %Ex. 10-4
rho_cool = 800;
del_T_del_rho = 3.876 %Linear Density Interpolation

%Length Constants
depth = 3;
L = 2.08;
pitch = .007374;
clad_gap = 0.00012;
clad_thickness = 0.00038;
R_f = 0.0029;
D_max_pipe = .3;
x = 0.024;

%Chosen Core Constants
total_desired_thermal_power = 500e6;
T_in = 653-273;
q_0 = 3500;
del_T = 300
num_rod = 73391;

%Chosen Hydraulic Constants
% m_dot = 1;
f = .001;
dz = 0.001

%%%%%%%%%%%%%%%%%%%%%%%%%%%%%%%%%%%%%%%%%%%%%%%%%%%%%%%%%%%%%%%%%%%%%%%%%%%%%%%%%%%%%%%%%%%%%%%%%%%%%%%%%%%%%%%%%%%%%%%%%%%%%%%%%%%%%%%%%%%%%%%%%%%%%%%%%%%%%%%%%%%%%%%%%%%%%%%%%%%%%%%%%%%%%%%%%%%%%%%%%%%%%%%%%%%%%%%%%%%%%%%%%%%%%%%%
%%%%%%%%%%%%%%%%%%%%%%%%%%
%Define empty arrays
%Define heat generation along fuel rod assuming cosine heat distribution
%  Eq. 13-14 Todreas
%Define Delta T across the core
%  Eq. 13-19 Todreas
%Define heat transfer coefficient as a function of height
%  Eq. 13-14 Todreas
%Define fuel centerline temperature
%  Eq 13-27 Todreas
%Define surface temperature along fuel rod
%  Eq 8-62 Todreas
%Define average temperature of fuel rod
%Define Bulk Coolant temperature as a function of height
%  Eq 13-18 Todreas
%Define inside cladding temperature as fuel surface temperature
%Define outer cladding temperature using 1-D Heat Conduction
%  Eq 13-22 Todreas
```

```
%%%%%%%%%%%%%%%%%%%%%%%%%%%%%%%%%%%%%%%%%%%%%%%%%%%%%%%%%%%%%%%%%%%%%%%%%%%%%%%%%
%Initial Calculations
z = [-L/2:dz:L/2];
h = [0:dz:L];
D_pipe = [.05:D_max_pipe*dz:D_max_pipe];
R_co = R_f + clad_gap + clad_thickness
R_ci = R_f + clad_gap
R_g = R_f + (.5)*clad_gap
% num_rod = total_desired_thermal_power/(q_0*L);
A_ht = R_co^2*pi*L
A_cool = pitch^2 - pi*R_co^2;
D_e = 4*A_cool/(2*pi*R_co)
Pe = rho_cool*(1)*D_e*c_p_cool/k_c;
Nu = 5 + .025*Pe^(4/5);
m_dot = (q_0*L*num_rod)/(pi*del_T*c_p_cool)
m_dot_channel = (q_0*L)/(pi*del_T*c_p_cool)
vel_cool = m_dot_channel/(rho_cool*A_cool)
% del_T = (q_0*L*num_rod)/(pi*m_dot*c_p_cool);

for i = 1:length(z)
   h_cool(i) = Nu*k_c/D_e;
   q(i) = q_0*cos(pi*z(i)/(L+x));
   A(i)=(L+x)/(pi*m_dot*c_p_cool)*(sin(pi*z(i)/(L+x))+sin(pi*L/(2*(L+x))));
   B(i) = (2*pi*R_co*h_cool(i))^(-1)+(2*pi*k_c)^(-1)*log(R_co/R_ci)+(2*pi*R_g*h_g)^(-1)+(4*pi*k_f)^(-1);
   T_cl(i) = T_in + q_0*(A(i)+(cos(pi*z(i)/(L+x))*B(i)));
   T_fo(i) = T_cl(i) - q(i)/(4*pi*k_f);
   T_avg(i) = q(i)/(8*pi*k_f)+T_fo(i);
   T_ci(i) = T_fo(i);
   D = (L+x)/(pi*m_dot*c_p_cool);
   E(i) = sin(pi*z(i)/(L+x))+sin(pi*L/(2*(L+x)));
   T_m(i) = T_in + q_0*D*E(i);
   F(i) = cos(pi*z(i)/(L+x))/(2*pi*R_co*h_cool(i));
   T_co(i) = T_in+q_0*(D*E(i)+F(i));
end

%%%%%%%%%%%%%%%%%%%%%%%%%%%%%%%%%%%%%%%%%%%%%%%%%%%%%%%%%%%%%%%%%%%%%%%%%%%%%%%%%
%Hot Channel Factors
%%%%%%%%%%%%%%%%%%%%%%%%%%%%%%%%%%%%%%%%%%%%%%%%%%%%%%%%%%%%%%%%%%%%%%%%%%%%%%%%%
q_avg = sum(q)/length(q);
axial_factor = max(q)/q_avg

%%%%%%%%%%%%%%%%%%%%%%%%%%%%%%%%%%%%%%%%%%%%%%%%%%%%%%%%%%%%%%%%%%%%%%%%%%%%%%%%%
%Natural Circulation
%%%%%%%%%%%%%%%%%%%%%%%%%%%%%%%%%%%%%%%%%%%%%%%%%%%%%%%%%%%%%%%%%%%%%%%%%%%%%%%%%
L_D = [0:5:5000];
for i = 1:length(L_D)
del_rho_cool(i) = (.5)*rho_cool*(vel_cool*.1)^2*f*(L_D(i))/(g*depth);
del_T_hr(i) = del_T_del_rho*del_rho_cool(i);
end

A_hr_core = total_desired_thermal_power/(sum(h_cool)*300/length(h_cool))
A_hr_sc = total_desired_thermal_power/(num_rod*sum(h_cool)*del_T_hr(101)/length(h_cool))
for i = 1:length(D_pipe)
   core_L_hr(i) = A_hr_core/(pi*D_pipe(i));
   sc_L_hr(i) = A_hr_sc/(pi*D_pipe(i));
end
%%%%%%%%%%%%%%%%%%%%%%%%%%%%%%%%%%%%%%%%%%%%%%%%%%%%%%%%%%%%%%%%%%%%%%%%%%%%%%%%%
%Pumping Power
%%%%%%%%%%%%%%%%%%%%%%%%%%%%%%%%%%%%%%%%%%%%%%%%%%%%%%%%%%%%%%%%%%%%%%%%%%%%%%%%%
for i = 1:length(L_D)
   pump_work(i) = m_dot*g*(depth+L + f*L_D(i));
end

%Format Plots to Kelvin
```

```
T_cl = T_cl + 273;
T_avg = T_avg  + 273;
T_fo = T_fo  + 273;
T_ci = T_ci  + 273;
T_co = T_co  + 273;
T_m = T_m + 273;

%Plots
 z = z + L/2;%Realign Core Hight to Base at Zero

figure(1)
plot(T_cl,z,T_avg,z,T_ci,z,T_co,z,'LineWidth',2)
grid on
xlabel('Temperature ( ^oK)')
ylabel('Position (m)')
legend('Centerline Temperature','Average Temperature','Fuel Surface/Inner Cladding Temperature','Cladding Outer Surface
Temperature','location','best')
title('Core Temperatures')

figure(2)
plot((T_m-653)*10^3,z,'LineWidth',2)
grid on
xlabel('Change in T_i_n - Coolant Temperature ( ^oK * 10^3)')
ylabel('Position (m)')
legend('Coolant Temperature',0)
title('Change in Core Temperatures T_i_n = 653^oK')

figure(3)
plot(del_rho_cool,L_D,'LineWidth',2)
grid on
xlabel('Delta Density ( Kg/ m^3)')
ylabel('Pipe L/D')
legend('Change in Density',0)
title('Natural Circulation')

figure(4)
semilogy(D_pipe*100, core_L_hr,D_pipe*100,sc_L_hr,'LineWidth',2)
grid on
xlabel('Diameter of Pipe (cm)')
ylabel('Length of Pipe Needed (m)')
title('Natural Circulation Heat Removal')
legend('Core','Single Channel',0)

figure(5)
plot(L_D, pump_work/1000,'LineWidth',2)
grid on
xlabel('Pipe L/D')
ylabel('Pump Power (kW)')
title('Pump Power Across Core')
```

Appendix I: Brandon Holden's MatLab Program

```
%%%%%%%%%%%%%%%%%%%%%%%%%%%%%%%%%%%%%%%%%%%%%%%%%%%%%%%%%%%%%%%%%
%Program to calculate various heat transfer activities in a liquid metal
%cooled modular fast reactor.
%
%Original Code written by NE 472 Senior Design Group:
% Jennifer Carney, Brandon Holden, Stephen Janson, Amy Scott,
% David Yancey, and Tom Young
%
%Edited and used by NE 472 Senior Design Group:
% Carol Dudney, Justin Belles, Brandon Davis, Michael Sharp, Stu Walker,
% and Laurel Helton
%%%%%%%%%%%%%%%%%%%%%%%%%%%%%%%%%%%%%%%%%%%%%%%%%%%%%%%%%%%%%%%%%

%Define Core Parameters

Qcore = 500e6;              % Thermal power output of core in watts (arbitrary)
pi = 3.14159;
Num = 68589;                    %Number of fuel elements
flength = 2.0828;               %Core height in meters
k_c = 21.5;                  %Cladding thermal conductivity (W/m * Kelvin)
k_f = 3.297;                      %fuel thermal conductivity (W/m * Kelvin)
h_g = 5700;                    %gap conductance (W/m * Kelvin)
R_co = .0068/2;                %cladding outer radius (m)
R_ci = .00604/2;                %cladding inner radius (m)
R_g = .00604/2;                 %radius of gap (between fuel and cladding) (in m)
core_diam = 2.25425*2;            %diameter of the core (m)
delta = 0.01;               %Extrapolation term
Le = flength + 2*delta*flength;     %Thermal Extrapolation length
pitch = .007374;                  %m
diameter = .0058;           %m
Ds = 0.001;                  %m (spacer diameter)
g = pitch/2;                 %in m (g is the spacing for the edge type fuel cell)
gs = g/2;                    %spacing for square pitch
Afp = (pi*(diameter^2))/4;   %Area of a fuel pin

%Coolant parameters (sodium)
k_cool = 62.9;               %coolant thermal conductivity (W/m*K)
c_p = 1230;                %specific heat capacity (J/kg*K)
rho = 968;               %density (kg/m^3)
mu = 2.27e4;               %Dynamic viscosity of sodium
Pr = (c_p*mu)/k_cool            %Prandtl number of sodium

%Universal Coolant parameters
Tcold = 653;                %Coolant inlet temperature (Kelvin)
corevelocity = .97;           %Velocity of coolant in the core (meters/second)


%Calculate linear heat transfer <q'_fe>
qlinear = Qcore/(Num*flength);        %W/m^3 per fuel pin

%Calculate maximum linear heat transfer <q'_femax>
qlinearMAX = (qlinear)*2;            %W/m^3 per fuel pin
```

```
%Calculate Area and hydraulic diameters of triangular and square channels
%(for design triangular is used)

Achannel=3^.5/2*pitch^2-pi*R_co^2/2;    %triangular channel area Achannel=3^.5/4*pitch^2-
pi*R_co^2/2;
%Achannel=pitch^2-(pi*R_co^2)/4;        %square channel area
Pwet=pi*R_co;                           %triangular wetted perimeter
%Pwet=2*pi*R_co;                        %square wetted perimeter

%Calculate hydraulic diameter
Dhyd=4*Achannel/Pwet;

%Calculate Reynold's Number
Re = (rho*Dhyd*corevelocity)/mu

%Calculate Peclet number
Pe = Re*Pr

%Calculate pitch to diameter ratio
ratio = pitch/diameter;

%Set up conditions to calculate Nusselt number
Nu = 1
if (ratio >= 1) & (ratio <= 1.5) & (Pe >= 10) & (Pe <= 5000)
   Nu = (-16.15 + 24.96*(pitch/diameter) - 8.55*((pitch/diameter)^2))*(Pe^0.3);
else if (ratio >= 1.25) & (ratio <= 1.95) & (Pe >=150) & (Pe <= 3000);
      Nu = 24.15*log10(-8.12 + 12.76*(pitch/diameter)-3.65*((pitch/diameter)^2))...
        + 0.0174*(1 - exp(6- 6*(pitch/diameter)))*((Pe-200)^0.9);
   end
end

%Caluclate heat transfer coefficient using Nusselt number
hcoolant = (Nu * k_cool)/Dhyd; %in units of W/(m^2 *K)

%Calculate mass flow rate of heated channel
mdot = rho*corevelocity*Achannel;

%Calculate maximum Core Temperatures
z=-Le/2:.01:Le/2;
jj=1;
for(ii=0:.01:Le);

%Maximum Fuel Centerline Temperature
Tcl(jj) = 1.05266*((Tcold) + qlinearMAX*(Le/(pi*mdot*c_p)*(sin(pi*z(jj)/Le) + sin(pi*flength/...
(2*Le)))+(1/(2*pi*R_co*hcoolant) + 1/(2*pi*k_c)*log(R_co/R_ci)+...
1/(4*pi*k_f))*cos(pi*z(jj)/Le)));

%Maximum Outer Radius Cladding Temperature
Tco(jj) = 1.05266*((Tcold) + (qlinearMAX)*((Le/(pi*mdot*c_p))*(sin((pi*z(jj))/(Le)) + sin((pi*flength)/...
(2*Le)))+(((1/(2*pi*R_co*hcoolant))*cos((pi*z(jj)/Le))))));

%Maximum Cladding Inner Radius Temperature
Tci(jj)=1.05266*((Tcold)+qlinearMAX*(Le/(pi*mdot*c_p)*(sin(pi*z(jj)/Le) + sin(pi*flength/(2*Le))...
   )+(1/(2*pi*R_co*hcoolant)+1/(2*pi*k_c)*log(R_co/R_ci))*cos(pi*z(jj)/(Le))));

%Maximum Coolant Temperature
Tcool(jj)=1.05266*((Tcold)+qlinearMAX*(Le/(pi*mdot*c_p)*(sin(pi*z(jj)/Le)+sin(pi*flength/(2*Le)))));
```

```
jj = jj+1;
end

%Make plot of fuel centerline temperature, outer cladding temperature,
%inner cladding temperature, and coolant temperature as function of fuel
%length position

plot(Tcl,z,Tco,z,Tci,z,Tcool,z)
grid
title ('Various Core Temperatures vs. Fuel Length Position')
legend('Fuel Centerline Temp','Outer Clad Temp','Inner Clad Temp','Coolant Temp')
xlabel('Temperature (K)')
ylabel('Cosine based core position')

%Send output to user
[m n] = max(Tcool);
fprintf('Max Coolant Temp is %f at position %f \n', m, z(n))
fprintf('Temperature Rise Across Core is %f \n', m - Tcold)

[m n] = max(Tco);
fprintf('Max Cladding Outer Temp is %f at position %f \n', m, z(n))

[m n] = max(Tci);
fprintf('Max Cladding Inner Temp is %f at position %f \n', m, z(n))

[m n] = max(Tcl);
fprintf('Max Fuel Centerline Temp is %f at position %f \n\n\n', m, z(n))
```

Appendix J: Design Project Definition

NE 472-572 Nuclear System Design
Spring 2007

Instructor: M.L. Grossbeck

Small Mobile Reactor for Underdeveloped Countries and Remote Locations

The objective of this project is to design a small reactor that can be transported by truck to a remote location. In addition to its small size, it will not be refueled on site but rather will be removed by truck and replaced with a reactor with a fresh core. Although the capacity remains to be chosen, 100 MW electric is a reasonable goal.

This project has considerable latitude it its design. Weight and size will probably make a pressure vessel impractical. However, a CANDU type design might be used with water as a coolant. Selection of the coolant will be a major design task left wide open. Liquid metals, gas, molten salt, or water will all be considered. The secondary plant must also be considered. However, the entire plant need not be delivered on a single truck; it might take several truck loads with a single load for the reactor at the time of refueling.

The reactor need not be thermal. We will also consider the advantages of a fast spectrum reactor using a liquid metal coolant.

Elements of Design

1. Power Coefficient and Void Coefficient

   Both of these coefficients are of utmost importance for operation and safety. Since most of our experience is with water reactors, consideration of other coolants will introduce us to a new regime. Fast reactors will also bring us into a new area. In all cases, we must have a negative void coefficient and a negative power coefficient.

2. Neutron transport

   This area will be important in evaluating the longevity of the fuel cycle, the power and void coefficients, and the flux profile. The small size is expected to aid in reactor control. The core geometry may be adjusted to optimize power coefficient and flux shape.

3. Heat Transfer

Thermal hydraulics will be considered not only for steady state heat removal but for decay heat removal upon shutdown or accident conditions. Many designs are available that enable natural circulation cooling under accident conditions. This will also be a consideration in our reactor.

4. Materials Selection

High temperature and high efficiency are not prime considerations. However, the more efficient, the smaller the reactor can be made. We must select materials that will withstand operating temperatures and the long fuel cycle. However, this is not a research project, only a conceptual design. We will identify areas for future research on materials or other requirements.

5. Secondary System

The secondary system will not be an area on which we will focus. However, we must identify the type of system and have an estimate of its size. Steam generators are very large. Perhaps another system will be more favorable.

6. Safety

Safety is always a consideration in a design project. For a remote reactor, it is a goal for it to operate with a minimum of intervention. Convection cooling in case of pump failure is a major advantage. Containment is essential. However, this will not be a major part of the design effort. Concepts that are already established can be used.

Course Objectives

1. Final Report

This is the main product of this effort. This is a conceptual design. We will determine the type of reactor, the coolant, fuel, size and shape. We will also identify areas for future research. We will not generate engineering drawings, and it will not be possible to make a complete design or even come close. However, a finished report showing the concept and showing no road blocks will be produced. It must be of sufficient quality that you will be willing to put your name on it and tell your supervisor and the nuclear community that this is your work and your recommendation. It will also constitute the major part of your course grade.

A selected final report from 472 and the report from 572 will each be entered into the American Nuclear Society Student Design Competition. If selected, one or two members of your team will be invited to attend the ANS meeting and present the results.

2. Final Oral Presentation

A member of each design team will make a presentation to the class on your product. This will be a team effort and will be graded. An oral presentation is a normal part of engineering that you will be expected to make many times as a practicing engineer.